DISCLOSURE

The research described in this article has not been subjected to each agency's policy review and therefore does not necessarily reflect their views, and no official endorsement should be inferred.

REFERENCES

(1) Schuster, D., Laggner, C., and Langer, T. (2005) Why drugs fail--a study on side effects in new chemical entities. *Curr. Pharm. Des. 11*, 3545–3559.

(2) Tropsha, A. (2010) Best practices for QSAR model development, validation, and exploitation. *Mol. Inf. 29*, 1868–1751.

(3) Hou, T., and Wang, J. (2008) Structure-ADME relationship: still a long way to go? *Expert Opin. Drug Metab. Toxicol. 4*, 759–770.

(4) Cui, Y., and Paules, R. S. (2010) Use of transcriptomics in understanding mechanisms of drug-induced toxicity. *Pharmacogenomics 11*, 573–585.

(5) Blomme, E. A., Yang, Y., and Waring, J. F. (2009) Use of toxicogenomics to understand mechanisms of drug-induced hepatotoxicity during drug discovery and development. *Toxicol. Lett. 186*, 22–31.

(6) Fielden, M. R., Brennan, R., and Gollub, J. (2007) A gene expression biomarker provides early prediction and mechanistic assessment of hepatic tumor induction by nongenotoxic chemicals. *Toxicol. Sci. 99*, 90–100.

(7) Zidek, N., Hellmann, J., Kramer, P. J., and Hewitt, P. G. (2007) Acute hepatotoxicity: a predictive model based on focused illumina microarrays. *Toxicol. Sci. 99*, 289–302.

(8) Hirode, M., Ono, A., Miyagishima, T., Nagao, T., Ohno, Y., and Urushidani, T. (2008) Gene expression profiling in rat liver treated with compounds inducing phospholipidosis. *Toxicol. Appl. Pharmacol. 229*, 290–299.

(9) Kiyosawa, N., Uehara, T., Gao, W., Omura, K., Hirode, M., Shimizu, T., Mizukawa, Y., Ono, A., Miyagishima, T., Nagao, T., and Urushidani, T. (2007) Identification of glutathione depletion-responsive genes using phorone-treated rat liver. *J. Toxicol. Sci. 32*, 469–486.

(10) Hirode, M., Horinouchi, A., Uehara, T., Ono, A., Miyagishima, T., Yamada, H., Nagao, T., Ohno, Y., and Urushidani, T. (2009) Gene expression profiling in rat liver treated with compounds inducing elevation of bilirubin. *Hum. Exp. Toxicol. 28*, 231–244.

(11) Uehara, T., Hirode, M., Ono, A., Kiyosawa, N., Omura, K., Shimizu, T., Mizukawa, Y., Miyagishima, T., Nagao, T., and Urushidani, T. (2008) A toxicogenomics approach for early assessment of potential non-genotoxic hepatocarcinogenicity of chemicals in rats. *Toxicology 250*, 15–26.

(12) Tamura, K., Ono, A., Miyagishima, T., Nagao, T., and Urushidani, T. (2006) Profiling of gene expression in rat liver and rat primary cultured hepatocytes treated with peroxisome proliferators. *J. Toxicol. Sci. 31*, 471–490.

(13) Zhu, H., Rusyn, I., Richard, A., and Tropsha, A. (2008) Use of cell viability assay data improves the prediction accuracy of conventional quantitative structure-activity relationship models of animal carcinogenicity. *Environ. Health Perspect. 116*, 506–513.

(14) Sedykh, A., Zhu, H., Tang, H., Zhang, L., Richard, A., Rusyn, I., and Tropsha, A. (2011) Use of in vitro HTS-derived concentration-response data as biological descriptors improves the accuracy of QSAR models of in vivo toxicity. *Environ. Health Perspect. 119*, 364–370.

(15) Uehara, T., Ono, A., Maruyama, T., Kato, I., Yamada, H., Ohno, Y., and Urushidani, T. (2010) The Japanese toxicogenomics project: application of toxicogenomics. *Mol. Nutr. Food Res. 54*, 218–227.

(16) Fourches, D., Muratov, E., and Tropsha, A. (2010) Trust, but verify: on the importance of chemical structure curation in cheminformatics and QSAR modeling research. *J. Chem. Inf. Model. 50*, 1189–1204.

(17) Kuz'min, V. E., Artemenko, A. G., and Muratov, E. N. (2008) Hierarchical QSAR technology based on the Simplex representation of molecular structure. *J. Comput.-Aided Mol. Des. 22*, 403–421.

(18) Varnek, A., Fourches, D., Horvath, D., Klimchuk, O., Gaudin, C., Vayer, P., Solov'yev, V., Hoonakker, F., Tetko, I. V., and Marcou, G. (2008) ISIDA: platform for virtual screening based on fragment and pharmacophoric descriptors. *Curr. Comput. Aided Drug Des. 4*, 191–198.

(19) Muratov, E. N., Artemenko, A. G., Varlamova, E. V., Polischuk, P. G., Lozitsky, V. P., Fedchuk, A. S., Lozitska, R. L., Gridina, T. L., Koroleva, L. S., Sil'nikov, V. N., Galabov, A. S., Makarov, V. A., Riabova, O. B., Wutzler, P., Schmidtke, M., and Kuz'min, V. E. (2010) Per aspera ad astra: application of Simplex QSAR approach in antiviral research. *Future. Med. Chem. 2*, 1205–1226.

(20) Tusher, V. G., Tibshirani, R., and Chu, G. (2001) Significance analysis of microarrays applied to the ionizing radiation response. *Proc. Natl. Acad. Sci. U.S.A. 98*, 5116–5121.

(21) Zheng, W., and Tropsha, A. (2000) Novel variable selection quantitative structure−property relationship approach based on the k-nearest-neighbor principle. *J. Chem. Inf. Comput. Sci. 40*, 185–194.

(22) Fan, R. E., Chen, P. H., and Lin, C. J. (2005) Working set selection using the second order information for training SVM. *J. Mach. Leaning Res. 6*, 1889–1918.

(23) Polishchuk, P. G., Muratov, E. N., Artemenko, A. G., Kolumbin, O. G., Muratov, N. N., and Kuz'min, V. E. (2009) Application of random forest approach to QSAR prediction of aquatic toxicity. *J. Chem. Inf. Model. 49*, 2481–2488.

(24) Marron, J. S., Todd, M. J., and Ahn, J. (2007) Distance weighted discrimination. *J. Am. Stat. Assoc. 102*, 1267–1271.

(25) Tropsha, A., and Golbraikh, A. (2007) Predictive QSAR modeling workflow, model applicability domains, and virtual screening. *Curr. Pharm. Des. 13*, 3494–3504.

(26) Golbraikh, A., and Tropsha, A. (2002) Beware of q2!. *J. Mol. Graphics Modell. 20*, 269–276.

(27) Tropsha, A., Gramatica, P., and Gombar, V. K. (2003) The importance of being earnest: validation is the absolute essential for successful application and interpretation of QSPR models. *Quant. Struct. Act. Relat. Comb. Sci. 22*, 69–77.

(28) Sedykh, A. Y., and Klopman, G. (2006) A structural analogue approach to the prediction of the octanol-water partition coefficient. *J. Chem Inf. Model. 46*, 1598–1603.

(29) Kovatcheva, A., Golbraikh, A., Oloff, S., Xiao, Y. D., Zheng, W., Wolschann, P., Buchbauer, G., and Tropsha, A. (2004) Combinatorial QSAR of ambergris fragrance compounds. *J. Chem. Inf. Comput. Sci. 44*, 582–595.

(30) Parviz, F., Matullo, C., Garrison, W. D., Savatski, L., Adamson, J. W., Ning, G., Kaestner, K. H., Rossi, J. M., Zaret, K. S., and Duncan, S. A. (2003) Hepatocyte nuclear factor 4alpha controls the development of a hepatic epithelium and liver morphogenesis. *Nat. Genet. 34*, 292–296.

(31) Luebke-Wheeler, J., Zhang, K., Battle, M., Si-Tayeb, K., Garrison, W., Chhinder, S., Li, J., Kaufman, R. J., and Duncan, S. A. (2008) Hepatocyte nuclear factor 4alpha is implicated in endoplasmic reticulum stress-induced acute phase response by regulating expression of cyclic adenosine monophosphate responsive element binding protein H. *Hepatology 48*, 1242–1250.

(32) Ji, C., and Kaplowitz, N. (2006) ER stress: can the liver cope? *J. Hepatol. 45*, 321–333.

(33) Lin, C. J., Malina, A., and Pelletier, J. (2009) c-Myc and eIF4F constitute a feedforward loop that regulates cell growth: implications for anticancer therapy. *Cancer Res. 69*, 7491–7494.

(34) Hirode, M., Omura, K., Kiyosawa, N., Uehara, T., Shimuzu, T., Ono, A., Miyagishima, T., Nagao, T., Ohno, Y., and Urushidani, T. (2009) Gene expression profiling in rat liver treated with various hepatotoxic-compounds inducing coagulopathy. *J. Toxicol. Sci. 34*, 281–293.

(35) Beyer, R. P., Fry, R. C., Lasarev, M. R., McConnachie, L. A., Meira, L. B., Palmer, V. S., Powell, C. L., Ross, P. K., Bammler, T. K., Bradford, B. U., Cranson, A. B., Cunningham, M. L., Fannin, R. D., Higgins, G. M., Hurban, P., Kayton, R. J., Kerr, K. F., Kosyk, O., Lobenhofer, E. K., Sieber, S. O., Vliet, P. A., Weis, B. K., Wolfinger, R., Woods, C. G., Freedman, J. H., Linney, E., Kaufmann, W. K., Kavanagh, T. J., Paules, R. S., Rusyn, I., Samson, L. D., Spencer, P. S., Suk, W., Tennant, R. J., and Zarbl, H. (2007) Multicenter study of acetaminophen hepatotoxicity reveals the importance of biological endpoints in genomic analyses. *Toxicol. Sci. 99*, 326–337.

(36) Rodgers, A. D., Zhu, H., Fourches, D., Rusyn, I., and Tropsha, A. (2010) Modeling liver-related adverse effects of drugs using knearest neighbor quantitative structure-activity relationship method. *Chem. Res. Toxicol. 23*, 724–732.

(37) Loew, G. H., and Goldblum, A. (1985) Metabolic activation and toxicity of acetaminophen and related analogs. A theoretical study. *Mol. Pharmacol. 27*, 375–386.

(38) Peters, J. M., Morishima, H., Ward, J. M., Coakley, C. J., Kimura, S., and Gonzalez, F. J. (1999) Role of CYP1A2 in the toxicity of long-term phenacetin feeding in mice. *Toxicol. Sci. 50*, 82–89.

(39) Aarbakke, J., Bakke, O. M., Milde, E. J., and Davies, D. S. (1977) Disposition and oxidative metabolism of phenylbutazone in man. *Eur. J. Clin. Pharmacol. 11*, 359–366.

(40) Porter, W. R., and Neal, R. A. (1978) Metabolism of thioacetamide and thioacetamide S-oxide by rat liver microsomes. *Drug Metab. Dispos. 6*, 379–388.

(41) Shen, M. L., Johnson, K. L., Mays, D. C., Lipsky, J. J., and Naylor, S. (2001) Determination of in vivo adducts of disulfiram with mitochondrial aldehyde dehydrogenase. *Biochem. Pharmacol. 61*, 537–545.

(42) Lee, P. W., and Neal, R. A. (1978) Metabolism of methimazole by rat liver cytochrome P-450-containing monoxygenases. *Drug Metab. Dispos. 6*, 591–600.

(43) Rechnagel, R. O., and Glende, E. A., Jr. (1973) Carbon tetrachloride hepatotoxicity: an example of lethal cleavage. *CRC Crit. Rev. Toxicol. 2*, 263–297.

(44) Kaufmann, P., Torok, M., Hanni, A., Roberts, P., Gasser, R., and Krahenbuhl, S. (2005) Mechanisms of benzarone and benzbromarone-induced hepatic toxicity. *Hepatology 41*, 925–935.

(45) Adam, W., Ahrweiler, M., Saha-Moller, C. R., Sauter, M., Schonberger, A., Epe, B., Muller, E., Schiffmann, D., Stopper, H., and Wild, D. (1993) Genotoxicity studies of benzofuran dioxetanes and epoxides with isolated DNA, bacteria and mammalian cells. *Toxicol. Lett. 67*, 41–55.

(46) Vassallo, J. D., Hicks, S. M., Daston, G. P., and Lehman-McKeeman, L. D. (2004) Metabolic detoxification determines species differences in coumarin-induced hepatotoxicity. *Toxicol. Sci. 80*, 249–257.

(47) Lake, B. G., Gray, T. J., Evans, J. G., Lewis, D. F., Beamand, J. A., and Hue, K. L. (1989) Studies on the mechanism of coumarin-induced toxicity in rat hepatocytes: comparison with dihydrocoumarin and other coumarin metabolites. *Toxicol. Appl. Pharmacol. 97*, 311–323.

(48) Felter, S. P., Vassallo, J. D., Carlton, B. D., and Daston, G. P. (2006) A safety assessment of coumarin taking into account species-specificity of toxicokinetics. *Food Chem. Toxicol. 44*, 462–475.

(49) Maggiora, G. M. (2006) On outliers and activity cliffs--why QSAR often disappoints. *J. Chem. Inf. Model. 46*, 1535.

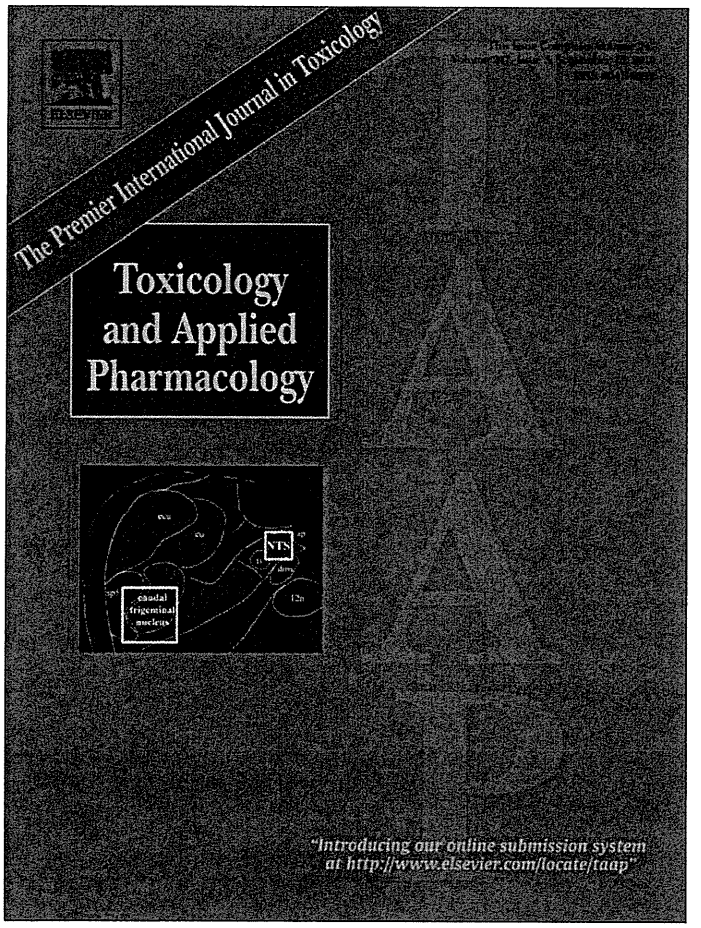

Toxicology and Applied Pharmacology 247 (2010) 211–221

Contents lists available at ScienceDirect

Toxicology and Applied Pharmacology

journal homepage: www.elsevier.com/locate/ytaap

Mechanism-based biomarker gene sets for glutathione depletion-related hepatotoxicity in rats

Weihua Gao [a,1], Yumiko Mizukawa [b,1], Noriyuki Nakatsu [a], Yosuke Minowa [a], Hiroshi Yamada [a], Yasuo Ohno [c], Tetsuro Urushidani [a,b,*]

[a] Toxicogenomics Informatics Project, National Institute of Biomedical Innovation, 7-6-8 Saito-Asagi, Ibaraki, Osaka 567-0085, Japan
[b] Department of Pathophysiology, Faculty of Pharmaceutical Sciences, Doshisha Women's College of Liberal Arts, Kodo, Kyotanabe, Kyoto 610-0395, Japan
[c] National Institute of Health Sciences, 1-18-1 Kamiyoga, Setagaya-Ku, Tokyo, 158-8501, Japan

ARTICLE INFO

Article history:
Received 15 February 2010
Revised 15 June 2010
Accepted 23 June 2010
Available online 16 July 2010

Keywords:
Biomarker
Glutathione depletion
Microarray
Toxicogenomics
Phorone

ABSTRACT

Chemical-induced glutathione depletion is thought to be caused by two types of toxicological mechanisms: PHO-type glutathione depletion [glutathione conjugated with chemicals such as phorone (PHO) or diethyl maleate (DEM)], and BSO-type glutathione depletion [i.e., glutathione synthesis inhibited by chemicals such as L-buthionine-sulfoximine (BSO)]. In order to identify mechanism-based biomarker gene sets for glutathione depletion in rat liver, male SD rats were treated with various chemicals including PHO (40, 120 and 400 mg/kg), DEM (80, 240 and 800 mg/kg), BSO (150, 450 and 1500 mg/kg), and bromobenzene (BBZ, 10, 100 and 300 mg/kg). Liver samples were taken 3, 6, 9 and 24 h after administration and examined for hepatic glutathione content, physiological and pathological changes, and gene expression changes using Affymetrix GeneChip Arrays. To identify differentially expressed probe sets in response to glutathione depletion, we focused on the following two courses of events for the two types of mechanisms of glutathione depletion: a) gene expression changes occurring simultaneously in response to glutathione depletion, and b) gene expression changes after glutathione was depleted. The gene expression profiles of the identified probe sets for the two types of glutathione depletion differed markedly at times during and after glutathione depletion, whereas Srxn1 was markedly increased for both types as glutathione was depleted, suggesting that Srxn1 is a key molecule in oxidative stress related to glutathione. The extracted probe sets were refined and verified using various compounds including 13 additional positive or negative compounds, and they established two useful marker sets. One contained three probe sets (Akr7a3, Trib3 and Gstp1) that could detect conjugation-type glutathione depletors any time within 24 h after dosing, and the other contained 14 probe sets that could detect glutathione depletors by any mechanism. These two sets, with appropriate scoring systems, could be promising biomarkers for preclinical examination of hepatotoxicity.

Introduction

Glutathione plays the main role in detoxifying electrophiles and scavenging free radicals (Lu, 1999), and consequently, glutathione depletion has been intensively investigated in relation to drug-induced hepatotoxicity. Many drugs such as acetaminophen overdose could elicit hepatotoxic effects through the depletion of glutathione in liver, and the events reflecting glutathione depletion have been considered as a potential biomarker of drug-induced hepatotoxicity (Soga et al., 2006).

Chemical-induced glutathione depletion has been reportedly caused mainly through two types of toxicological mechanisms: a) conjugation-type glutathione depletion, i.e., glutathione is conjugated with chemicals such as phorone (PHO; van Doorn et al., 1978) or diethylmaleate (DEM; Plummer et al., 1981), and b) glutathione depletion by inhibition of glutathione biosynthesis with an enzyme inhibitor, such as L-buthionine-(S,R)-sulfoximine (BSO; Griffith, 1981). The former type is similar to the hepatotoxic mechanism of acetaminophen overdosing, where activated metabolites such as NAPQI deplete glutathione by forming a conjugate with glutathione and then it is excreted from hepatocytes (Dahlin et al., 1984). Previously, 69 gene probe sets of the Rat Genome U34A GeneChip (Affymetrix, Inc.) were identified as glutathione depletion-responsive genes in liver using BSO (Kiyosawa et al., 2004), and later 161 gene probe sets of the RAE 230A GeneChip (Affymetrix, Inc.) were reported using phorone (PHO) as a glutathione-depleting agent (Kiyosawa et al., 2007). Interestingly, common genes between the two above studies were scarce, suggesting that genes with

* Corresponding author. Department of Pathophysiology, Faculty of Pharmaceutical Sciences, Doshisha Women's College of Liberal Arts, Kodo, Kyotanabe, Kyoto 610-0395, Japan. Fax: +81 72 641 9850.
E-mail address: turushid@dwc.doshisha.ac.jp (T. Urushidani).
[1] These authors contributed equally to this work.

0041-008X/$ – see front matter © 2010 Elsevier Inc. All rights reserved.
doi:10.1016/j.taap.2010.06.015

different functions were selected based on differing glutathione-depleting mechanisms. Another possibility is that the difference was due to the different protocols. BSO was given to rats in drinking water for 4 days and PHO was given once to rats; the animals were euthanized within 24 h, suggesting that the gene expression changes in the former were due to cell damage after long-term glutathione depletion. Furthermore, the latter reflected the events during and/or shortly after glutathione depletion. Other problems of these studies were that they both extracted exclusively upregulated genes and that both used an old version of the GeneChip, meaning that significant genes might have been overlooked. Moreover, the lists contained a large number of genes, most of which could not explain that the mechanism of events were due to glutathione depletion. These facts raised concern regarding the usefulness of gene sets as biomarkers, especially for elucidating toxicological mechanisms.

Considering the arguments presented above, we performed experiments using a new strategy in order to extract genes with mechanism-based, glutathione depletion-related expression changes. We then examined the validity of the gene lists on several compounds in our transcriptome database, TG-GATEs (Urushidani, 2007), to establish useful biomarkers for preclinical toxicity examination.

Materials and methods

Chemicals. The compounds used in this study are listed in Table 1 with their names, abbreviations, doses, administration routes, and vehicles. Conjugation-type glutathione depletors, PHO, 40, 120, 400 mg/kg, and DEM, 80, 240, 800 mg/kg were employed. BSO, 150, 450, 1500 mg/kg was used as a glutathione synthetase inhibitor. These three compounds were intraperitoneally (i.p.) administered to rats. For positive compounds such as glutathione depletors, bromobenzene (BBZ; van Doorn et al., 1978), acetaminophen (APAP, van Doorn et al., 1978), coumarin (CMA; Lake et al., 1989), methapyrilene (MP; Ratra et al., 2000), nitrofurazone (NFZ; Sorrentino et al., 1987), ethionine (ET; Waterfield et al., 1998), and thioacetamide (TAA; Mesa et al., 1996) were selected. Of these, the first five (BBZ, APAP, CMA, MP and NFZ) are classified as conjugation-type, whereas the remaining two are nonconjugation-types, i.e., ET is considered to be an enzyme synthesis inhibitor, and TAA is postulated to increase the ratio of oxidized glutathione. As negative compounds, erythromycin (EME), gentamicin (GMC), glibenclamide (GBC), hexachlorobenzene (HCB), isoniazid (INAH), penicillamine (PEN) and perhexiline (PH) were employed. The highest dose of each compound was selected based on a 7-day repeated preliminary study. Except for gentamicin, which was given intravenously, all compounds were administered orally to rats dissolved or suspended in 5% methylcellulose or corn oil as indicated in Table 1.

Animal treatment. The animal experiments were carried out according to the standard protocol in our project as previously described (Urushidani, 2007; Kiyosawa et al., 2007). Briefly, five-week old male Crl:CD(SD) rats were purchased from Charles River Japan Inc. (Kanagawa, Japan). The animals were individually maintained in stainless-steel cages in a temperature- and humidity-controlled environment (21–25 °C, 40–70% relative humidity, 12-h light/dark cycle) for 1-week quarantine and nonexposure periods. All animals had access to water and food *ad libitum*, and fasting was not applied before euthanasia. Animals (n = 5 per group) were randomly assigned and administered a single dose of the test compound or matched vehicle control as listed in Table 1. Blood samples were collected for biochemical assay in tubes containing heparin lithium 3, 6, 9 or 24 h after treatment. Activities of alanine aminotransferase (ALT) and aspartate aminotransferase (AST) in plasma were determined using a 7080 Clinical Analyzer (Hitachi High-Technologies Corporation, Tokyo, Japan). The animals were then euthanized and the livers were removed and soaked in RNA*later* (Ambion, Austin, TX, USA) immediately after sampling and stored at −80 °C until use for gene expression analysis. In animals treated with PHO, DEM, BBZ (high dose only) and BSO or matched vehicle, another aliquot of liver sample was immediately frozen in liquid nitrogen for measurement of hepatic glutathione contents. The remaining liver samples were fixed in 10% neutral buffered formalin for histopathological examination. All experimental procedures were conducted in accordance with Guidelines for Proper Conduct of Animal Experiments issued by the Science Council of Japan and with the approval of the Ethics Review Committee for Animal Experimentation of the National Institute of Health Sciences.

Histopathology. The fixed liver samples were dehydrated through graded alcohols and embedded in paraffin. Serial sections of 2–3-μm thickness were stained with hematoxylin and eosin for pathological examination.

Measurements of hepatic glutathione content. The liver samples (0.1 g) were homogenized with 5% 5-sulfosalicylic acid (Sigma-

Table 1
Compounds.

Compounds	Abbreviation	Dose (mg/kg)			Administration route	Vehicles
		Low	Middle	High		
Positive						
Phorone	PHO	40	120	400	IP	Corn oil
Diethyl maleate	DEM	80	240	800	IP	Corn oil
Bromobenzene	BBZ	30	100	300	PO	Corn oil
Acetaminophen	APAP	300	600	1000	PO	5% MC
Coumarin	CMA	15	50	150	PO	Corn oil
Methapyrilene	MP	10	30	100	PO	5% MC
Nitrofurazone	NFZ	30	100	300	PO	5% MC
Buthionine sulfoximine	BSO	150	450	1500	IP	Saline
Ethionine	ET	25	80	250	PO	5% MC
Thioacetamide	TAA	4.5	15	45	PO	5% MC
Negative						
Erythromycin	EME	100	300	1000	PO	5% MC
Gentamicin	GMC	10	30	100	IV	Saline
Glibenclamide	GEC	100	300	1000	PO	Corn oil
Hexachlorobenzene	HCB	300	1000	2000	PO	Corn oil
Isoniazid	INAH	200	600	2000	PO	5% MC
Penicillamine	PEN	100	300	1000	PO	5% MC
Perhexiline	PH	15	50	150	PO	5% MC

MC: methyl cellulose; PO: peroral; IP: intraperitoneal; IV: intravenous.

Aldrich) and centrifuged at 12,000 rpm for 10 min at 4 °C. The supernatant was used for measurement of total glutathione content in the liver using the Total Glutathione Quantification Kit (Dojindo Laboratories), according to the manufacturer's instructions. Using this kit, total glutathione content was measured without distinguishing the oxidized/reduced level.

GeneChip analysis. Microarray analysis was carried out using GeneChip® RAE 230 2.0 probe arrays (Affymetrix) on three out of five samples in each dosing group for rat liver samples. Sample preparation and processing procedure was performed as described in detail in the Affymetrix standard protocol and our prior publications (Kiyosawa et al., 2007). The digital image files were processed by Affymetrix Microarray Suite ver. 5.0 (MAS, Affymetrix). Microarray image data were analyzed with GeneChip Operating Software (Affymetrix). All microarray intensities were normalized for each chip by adjusting the mean intensity to 500 (per chip normalization). The microarray data used in this study is available upon request from the corresponding author (turushid@dwc.doshisha.ac.jp).

Microarray data analysis. Our strategy is summarized and illustrated in Fig. 1. To identify differentially expressed probe sets in response to glutathione depletion induced by the two above mentioned mechanisms, i.e., conjugation-type (PHO and DEM) and enzyme inhibition-type (BSO), we focused on the following two time courses of changes for the two types of mechanisms for glutathione depletion: a) gene expression changes at the time when glutathione was depleted (designated "During" in Fig. 1), and b) gene expression changes due to the events after glutathione depletion ("After" in Fig. 1). For the identification of probe sets in the first case "During", both Spearman's and Pearson's correlation coefficients between the signal value and hepatic glutathione content were calculated for all probe sets from PHO and DEM-treated rat livers 3 h after treatment with all of the doses and the vehicle. Calculations were also performed for BSO-treated rat livers 6 h after treatment because the peaks of glutathione depletion were observed at 3 and 6 h after treatment. The probe sets having a $p<0.05$ value for either Spearman's or Pearson's correlation coefficient were considered as being correlated with the glutathione content. In this way, both positive and negative correlations were detected. Secondly, the fold change in the ratio of the geometric means of the expression intensities in treated and control samples were then calculated, and a two-sided Welch's t-test was performed. The probe sets having three Affymetrix "present calls" in either the treated or control groups, as well as having expression values of at least 1.5-fold greater or 0.67-fold less than the control were chosen from mid or high dose PHO- and BSO-treated samples and high dose DEM-treated rat ($p<0.05$). Significant reduction of glutathione content was observed. As we needed additional compounds for gene selection, we used BBZ, which reportedly causes glutathione depletion (van Doorn et al., 1978). The ability of BBZ to do this was confirmed, and then the probe sets with the same criteria were extracted for PHO treatment. The probe sets extracted from PHO-treated rats were then refined by choosing those that were also commonly changed in DEM- and BBZ-treated rats (designated as Marker I in Fig. 1). The probe sets extracted from BSO-treated rats were then refined by choosing significant genes as described in the next section (designated as Marker II in Fig. 1).

To identify the probe sets in the second "After" condition, the probe sets having three Affymetrix "present calls" in either treated or control groups, as well as a fold change ratio of greater than 1.5-fold or less than 0.67-fold were selected at 6, 9, and 24 h after being treated with middle or high doses of PHO ($p<0.05$) and DEM ($p<0.1$), or 9 and 24 h after being treated with BSO ($p<0.05$), because the peaks of glutathione depletion were observed at 3 and 6 h after treatment. The p value for DEM was doubled in order to reduce beta errors, considering that reduction of glutathione by DEM was much less than that by PHO or BSO. Secondly, the probe sets that were common at three sampling points, i.e., 6, 9 and 24 h for both PHO- and DEM-treated samples, were identified as responsive genes to the events after glutathione depletion induced by conjugation-type glutathione depletion (designated as Marker III in Fig. 1). The probe sets commonly expressed at 9 and 24 h for BSO-treated samples were

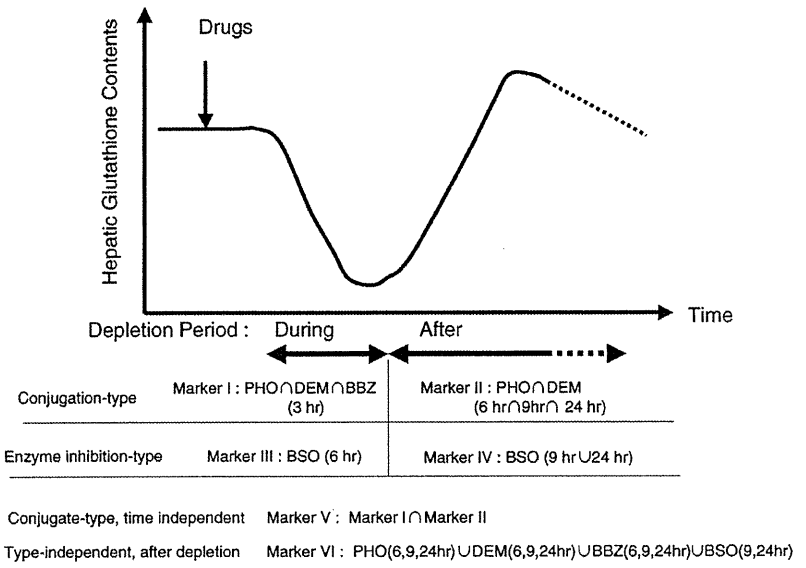

Fig. 1. Schematic representation of the strategy for biomarker gene extraction. The upper graph illustrates the typical pattern of hepatic glutathione content after the administration of two types of glutathione depletors, i.e., conjugation and enzyme inhibition-types. After dosing, the content decreases and then recovers with time. In some cases, it increases over the normal level. In this study, analyses were done in two periods for each type. One was the time when glutathione was depleted ("During") and the other was the time after the peak of depletion ("After"). Glutathione depletion occurred at 3 h by PHO, DEM and BBZ, whereas it occurs at 6 h after BSO, and thus, the corresponding periods differed between compounds. For each time and type, featured genes were extracted and designated as Markers I to IV. Time- and type-independent markers (V and VI) were also obtained by combination of the gene lists.

identified as responsive genes to the events after glutathione depletion induced by enzyme inhibition-type glutathione depletion (designated as Marker IV in Fig. 1).

In the next step, commonly expressed probe sets were chosen from the "During" and "After" scenarios. We considered them as robust biomarkers in response to events induced by glutathione depletion independent on the assay period. This strategy was effective for conjugation-type glutathione depletion. Marker V was obtained by taking the intersection of Marker I and Marker III (Fig. 1). However, it was not effective for enzyme inhibition-type depletion because the intersection of Markers II and IV was vacant. In another step, we tried to obtain markers responsive to glutathione depletion that was independent of the depletion type. To do this, we combined the "After" probe sets between conjugation- and enzyme inhibition-types, i.e., PHO (6, 9, and 24 h), DEM (6, 9 and 24 h), BBZ (6, 9, and 24 h) and BSO (9 and 24 h). As these contained too many probe sets, we refined these sets with principal component analysis (PCA) using 17 reference compounds to get 14 probe sets designated as Marker VI in Fig. 1.

Verification of the identified probe sets. The various identified probe set lists relating to glutathione depletion were verified using gene expression data from rat liver treated with the 13 additional positive or negative glutathione-depleting compounds (Table 1) in our database, TG-GATEs (genomics assisted toxicity evaluation system developed by Toxicogenomics Project, Japan; Urushidani, 2007). First, we verified the obtained lists by PCA when the classification was reasonable. Visualization of the data was performed by Spotfire® DecisionSite for Functional Genomics 9.1.1 (Spotfire).

To facilitate analysis in the large-scale microarray data, a simple one-dimensional score (TGP1 score) was developed to visualize the expression tendency as a whole for all of the identified probe sets in a certain group (Kiyosawa et al., 2006). The TGP1 score was calculated as follows: the signal log ratio was calculated by dividing the mean signal value of a treated group by that of the corresponding control. First, the sum of the signal log ratios for the used probe sets was calculated, and then divided by the number of probe sets used (Index 1). Next, the sum of the squared signal log ratios for the used probe sets was calculated, and then divided by the number of probe sets used (Index 2). Finally, the TGP1 score was calculated by multiplying Index 1 with Index 2. This scoring system is convenient for comparing the response of a gene group to exposure by various compounds. In this way, the TGP1 score was calculated for the refined lists of the identified probe sets, which were identified as candidate gene biomarkers for glutathione depletion in all 17 compounds.

Results

Plasma biochemistry and histopathology

As representative markers of hepatotoxicity, ALT and AST were measured. Although there were significant increases in the serum enzyme levels from treated animals; increases at least two times greater than the control were only observed in groups treated with the highest doses of BBZ, PHO and TAA at 24 h. This means that secondary changes due to cell injury could be excluded when considering time and dose points other than the highest doses of these three compounds at 24 h. APAP, MP and GBC showed significant increases in AST or ALT with the highest dose, but their increments were less than twice that of the control, suggesting that most of the tested compounds did not cause drastic cellular damage within 24 h, even at the highest dose.

We confirmed these observations by histopathological examination. Excluding minimal changes, some changes were noticed with the highest dose at 24 h after dosing. Inflammatory infiltration was observed in PHO, APAP, MP, ET and TAA. Necrosis was found in MP and TAA. Eosinophilic changes were observed in PHO, APAP, MP, ET and TAA. DEM induced "increased mitosis" with the highest dose at 3 and 6 h after dosing, whereas no such changes were observed at any other dose or time points. Our histologist considered that these changes were not related to drug effects because the changes were graded as "minimal" or "slight" and transient in the earliest time points. Reviewing our database, all these compounds showed various types of hepatotoxicity up to 28 days of repeated administration except for GMC and PEN, which did not produce any histological changes in rat livers but caused obvious damage in rat kidneys (data not shown).

Glutathione content in treated rat liver

The glutathione content in rat livers after a single dose of PHO, DEM or BSO is shown in Fig. 2. Hepatic glutathione content was decreased compared with the control for all three standard compounds. They were significantly decreased to 1/20 and 1/3 of the control value 3 h after treatment with the high doses of PHO and DEM, respectively. They then gradually recovered by 6 and 9 h after treatment, surpassing the control level by 24 h after treatment. In the case of BSO, the decrease in hepatic glutathione content occurred significantly later, i.e., the peak reduction was 6 or 9 h after treatment, and it recovered to the control level 24 h after treatment. Therefore, to control for changes in the extraction of genes when glutathione was depleted, we chose the expression data at the sampling time point: 3 h for PHO and 6 h for BSO. With regard to case b) when extraction of genes changed after glutathione depletion, the data at the sampling time at 6, 9, and 24 h after treatment for PHO and DEM were used, but the used data were at 9 and 24 h after treatment for BSO.

To make the gene selection, we needed another standard glutathione depletor to get reasonable results (see below). We then checked total glutathione content in liver treated with BBZ (high dose only) and found marked glutathione depletion with a similar time course to that of BSO (Fig. 2).

Identification of differentially expressed gene probe sets in response to glutathione depletion in rat liver

In the first step of genes extraction (simultaneously responding to conjugation-type glutathione depletion), probe sets whose changes were significantly correlated with glutathione contents from 3 to 24 h after PHO- or DEM-treatment were extracted and filtered, resulting in 912 probe sets from the PHO-treated samples and 250 probe sets from the DEM-treated samples. Of all of these probe sets, 73 sets were found to be common to both PHO- and DEM-treated groups at 3 h after treatment. As it was still a large number, we needed another standard compound. As stated above, we confirmed that BBZ actually caused marked glutathione depletion. Using this additional data, 25 probe sets were selected out of the 73 by taking the commonly mobilized genes in the BBZ-treated group at 3 h. We considered them as genes that were simultaneously responding to conjugation-type glutathione depletion at the time when glutathione was depleted (Marker I in Fig. 1; gene list is shown in Supplemental Table 1). Using these 25 probe sets, PCA was performed on the expression data of the 17 compounds at 3 h (Supplemental Fig. 1). It appears that most of the conjugation-type drugs, i.e., CMA, NFZ, MP, DEM and PHO, were well separated from controls and nonconjugation-type drugs, i.e., BSO, TAA and ET, whereas the separation of the typical conjugation-type drugs, APAP and BBZ, was relatively small. The latter observation was considered to be due to their time course such that the onset of changes in these two appeared to be a bit later.

For enzyme inhibition-type glutathione depletion, 141 probe sets were selected from the data of rat liver at 6 h after BSO treatment. As we had little knowledge about specific inhibitors of glutathione

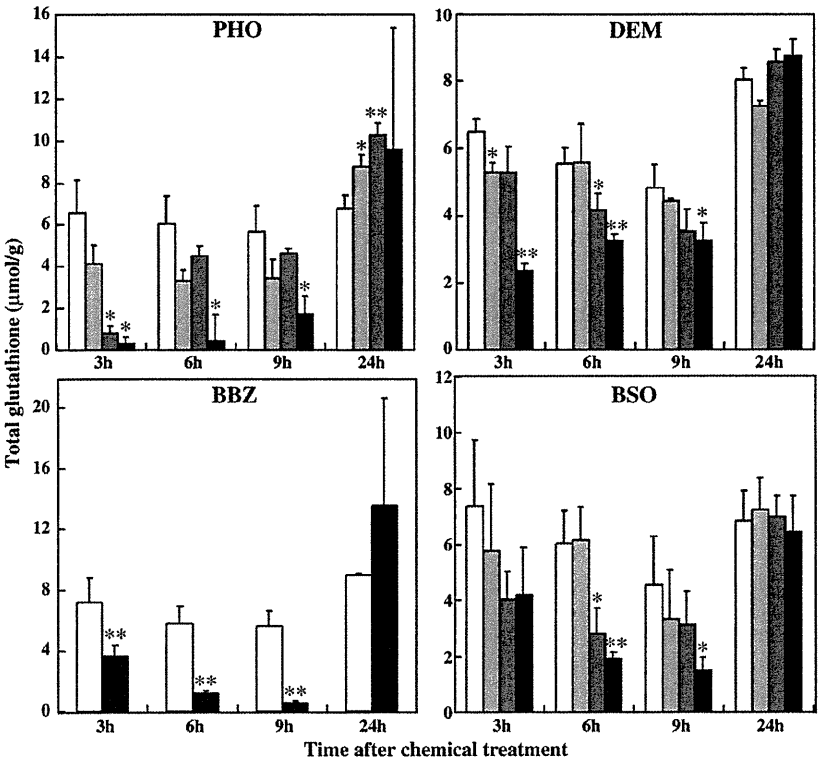

Fig. 2. Hepatic glutathione content after treatment with phorone (PHO, 40, 120, and 400 mg/kg, i.p.), diethylmaleate (DEM, 80, 240, and 800 mg/kg, i.p.), L-buthionine-(S,R)-sulfoximine (BSO, 150, 450, and 1500 mg/kg, i.p.), or bromobenzene (BBZ, 300 mg/kg, p.o.). Rats were treated with the compounds or vehicle, and the livers were removed 3, 6, 9 and 24 h after treatment. Hepatic total glutathione content was measured, and the data are presented as the mean ± S.D. (n = 3). ** and *, $p<0.01$ and $p<0.05$ by Student's test, respectively. □, vehicle; ▒, low dose; ▓, middle dose; ■, high dose.

synthesis, we used 17 selected compounds for refinement. We performed PCA on these compounds using the 141 probe sets and obtained a relatively reasonable separation (data not shown). In order to exclude insignificant genes, the probe sets with eigenvector values that were within the top 10% of the total were selected, resulting in 14 probe sets consisting of 6 upregulated and 8 downregulated ones (Marker II in Fig. 1; gene list is shown in Supplemental Table 2). Using these 14 probe sets, PCA was performed on the expression data at 6 h after dosing, and we obtained similar results to that using 141 probe sets (Supplemental Fig. 3). In contrast to the PCA using conjugation-type markers, BSO and TAA were well separated from controls. On the other hand, the separation of conjugation-type compounds was much better than that of BSO and TAA. Although ET was enrolled as a positive compound, it was classified as negative by the PCA results.

In order to extract genes that were mobilized after conjugation-type glutathione depletion, commonly expressed probe sets at 6, 9 and 24 h after treatment in both PHO- and DEM-treated rat livers were selected, and 21 probe sets were similarly selected because of their response to hepatotoxicity after glutathione depletion (Marker III in Fig. 1; gene list is shown in Table 2). The content of the list appeared to be quite different from those of 25 probe sets that were mobilized during glutathione depletion. Of the extracted genes after glutathione depletion, there were nine upregulated ones, of which only Akr7a3 and Trib3 were also found in the list of "During" markers, i.e., Marker I. Using Marker III, PCA was performed on the expression data at 24 h after dosing of 17 compounds (Supplemental Fig. 3). All of the conjugation-type drugs were well separated from controls with a high PC1 contribution rate (89.4%). Of the nonconjugation-type compounds, TAA showed a slight separation from its controls, whereas BSO and ET remained in the cluster of controls.

In the case of enzyme inhibition-type glutathione depletion, combining the 9- and 24-h time points after BSO treatment allowed 22 probe sets to be selected as marker genes that responded to hepatotoxicity after inhibition of glutathione synthesis (Marker IV in Fig. 1; gene list is shown in Table 3). In contrast to that of conjugation-type Marker III in Table 2, genes encoding transporters and other genes in various categories were significantly mobilized. PCA was performed on the expression data at 24 h using these probe sets as shown in Supplemental Fig. 4. It appeared that the most of the positive compounds are separated from the controls, but their separation was relatively unclear. These probe sets were considered to be of the nonconjugation rather than the conjugation-type because DEM localized within the control cluster and there was no clear separation between the two types.

In Marker I ("During" of conjugation-type), only three probe sets were found to overlap with Marker III ("After" of conjugation-type) in Table 2. These three probe sets, i.e., Akr7a3, Trib3 and Gstp1 (Marker V in Fig. 1; denoted by the asterisk in the last column of Table 2) were considered as the most robust gene biomarker candidates in response to hepatotoxicity induced by glutathione depletion through glutathione conjugation regardless of the time range. Using PCA, these three probes successfully separated conjugation-type compounds with a high contribution rate (97.2%) of PC1 (Fig. 3). Of the nonconjugation-type compounds, BSO and TAA tended toward the PC1 direction.

In order to extract gene biomarker candidates in response to hepatotoxicity induced by glutathione depletion regardless of the depletion mechanism, the union of the probe sets mobilized after treatment with PHO/DEM/BBZ and BSO was used, and 43 probe sets were obtained. To refine these 43 probe sets, PCA was performed on the expression data of the 17 compounds, and 14 probe sets with

Table 2
List of genes that were mobilized after conjugation-type glutathione depletion.

	Probe set ID	Gene name	Gene symbol	
*	1368009_at	Glucosamine	Gne	
*	1368036_at	Protein tyrosine phosphatase, receptor type, F	Ptprf	
*	1368121_at	Aldo-keto reductase family 7, member A3 (aflatoxin aldehyde reductase)	Akr7a3	*
	1369093_at	Reelin	Reln	
*	1370030_at	Glutamate cysteine ligase, modifier subunit	Gclm	
	1370599_a_at	Protein tyrosine phosphatase, receptor type, D	Ptprd	
*	1370688_at	Glutamate-cysteine ligase, catalytic subunit	Gclc	
	1372604_at	Similar to apolipoprotein L2; apolipoprotein L-II (predicted)	RGD1309808_predicted	
*	1372889_at	Transcribed locus	–	
	1376990_at	Transcribed locus	–	
*	1377013_at	–	–	
*	1379900_at	Transcribed locus	–	
*	1381968_at	Cellular repressor of E1A-stimulated genes 1	Creg	
	1382544_at	Transcribed locus	–	
*	1383425_at	Complement component 5	C5	
	1386321_s_at	Tribbles homolog 3 (*Drosophila*)	Trib3	*
*	1388122_at	Glutathione-S-transferase, pi 1	Gstp1	*
*	1388416_at	Low density lipoprotein receptor-related protein 1	Lrp1	
*	1388425_at	OAF homolog (*Drosophila*)	Oaf	
	1388911_at	DNA primase, p58 subunit	Prim2	
	1390692_at	Cytidine 5′-triphosphate synthase (predicted)	Ctps_predicted	

Shade on the column indicates that the gene was downregulated. Others were generally upregulated after glutathione depletion. These genes are designated as Marker III in Fig. 1. Only three probe sets (indicated by asterisks on the far right of the table) are also included in the probe sets that were extracted as those simultaneously responding to conjugation-type glutathione depletion (Marker I).
Probes with an asterisk on the left side of the table were selected as follows: the union of the probe sets mobilized after treatment with PHO/DEM/BBZ and BSO was taken, and PCA was performed using 43 probe sets and the probes with eigenvector values of the top 30% were selected. Of the finally obtained 14 probe sets, 13 were from this table (conjugation-type), whereas one was from the other type (Table 3). These 14 probe sets are designated as Marker VI in Fig. 1.

Table 3
List of genes that were mobilized after enzyme inhibition-type glutathione depletion.

	Probe set ID	Gene name	Gene symbol
	1369840_at	Integral membrane transport protein UST4r	UST4r
	1372613_at	3-hydroxybutyrate dehydrogenase, type 2 (predicted)	Bdh2_predicted
	1373043_at	Stromal cell-derived factor 2-like 1 (predicted)	Sdf2l1_predicted
	1377472_at	Exostoses (multiple)-like 1 (predicted)	Extl1_predicted
	1378131_at	Similar to solute carrier family 9 (sodium/hydrogen exchanger), isoform 9 (predicted)	RGD1560736_predicted
	1379967_at	Zinc finger protein 367	Zfp367
	1379989_at	Similar to Antxr2 protein	LOC305633
	1380262_at	Transcribed locus	–
	1383401_at	Testis derived transcript	Tes
	1384312_at	Iroquois related homeobox 1 (*Drosophila*) (predicted)	Irx1_predicted
	1384380_at	Transcribed locus	–
	1385398_at	Zinc finger and BTB domain containing 7B (predicted)	Zbtb7b_predicted
	1386261_x_at	Caveolin 2	Cav2
*	1387022_at	Aldehyde dehydrogenase 1 family, member A1	Aldh1a1
	1389581_at	Interleukin 33	Il33
	1390507_at	Interferon stimulated exonuclease 20	Isg20
	1391848_at	RNA binding motif protein 27 (predicted)	Rbm27_predicted
	1393857_at	Transcribed locus	–
	1394488_at	Transcribed locus	–
	1394570_at	Kell blood group precursor (McLeod phenotype) homolog	Xk
	1395547_at	Transcribed locus	–
	1396419_at	–	–

Shade on the column indicates that the gene was downregulated. Others were generally upregulated after glutathione depletion. These genes are designated as Marker IV in Fig. 1. The probe with an asterisk on the left of the table was selected as follows: the union of the probe sets mobilized after treatment of PHO/DEM/BBZ and BSO was taken, and PCA was performed using obtained 43 probe sets, and probes with eigenvector values of the top 30% were selected. Of the finally obtained 14 probe sets, only one was from this table (enzyme inhibition-type), whereas others were from the other type (Table 2). These 14 probe sets are designated as Marker VI in Fig. 1.

eigenvector values that were within the top 30% of the total were selected (Marker VI in Fig. 1; denoted by the asterisk in the first column of Tables 2 and 3). Of the 14 probes, only one, Aldh1a1, was derived from the BSO data, whereas all of the other 13 probe sets were from the conjugation-type glutathione depletion group. PCA using these 14 probe sets also successfully separated the positive compounds with a high contribution rate (86.5%) of PC1 (Fig. 4). With this PCA, all of the positive compounds were separated, although the separation of ET was not toward the PC1 but the PC2 direction.

Verification of the identified probe sets in response to glutathione depletion-related hepatotoxicity

The last two lists, i.e., Marker V (Akr7a3, Trib3 and Gstp1; conjugation-type marker, time-independent) and Marker VI (general glutathione depletion marker, time-independent) appeared to be promising candidates. Their usefulness was verified using our scoring system, the TGP1 score, and shown as heatmaps in Fig. 5. Fig. 5A shows the TGP1 scores using Marker V. All of the conjugation-type positive compounds (magenta in the figure) are clearly distinguished by their high values from nonconjugation-type positive (orange) and negative (white) compounds. Of the nonconjugation-type compounds, TAA showed a slightly high score at 24 h. It is noteworthy that all of the conjugation-type compounds were determined to be positive at 24 h because the upregulation of these three genes was sustained during and after glutathione depletion.

For Marker VI, the TGP1 scoring system is not suitable as is because it only works when the direction of the change of each marker gene in the list is uniform. We then separately calculated the score for 6 up- and 8 downregulated ones out of 14 probe sets. As is obvious from Fig. 5B, all of the glutathione-depleting compounds could be distinguished from the negative ones, although the values of ET and BSO were relatively low and became highly positive only at 24 h. TGP1 scores could be calculated for the remaining eight downregulated probe sets; however, the separation was not as good as the six upregulated ones (Fig. 5C).

In order to show the dose dependency of the expression changes of the candidate genes, expression changes caused by PHO or BSO in Marker V, Akr7a3, Trib3 and Gstp1, are depicted in Supplemental Fig. 5. Their expression profiles could differentiate them from other compounds by the presence of excellent time and dose dependencies. Therefore, these three probe sets are expected to be produce reproducible results in toxicological examinations.

Discussion

In this study, we employed the following protocol in order to obtain robust mechanism-based biomarker gene lists that could identify glutathione depletion (Fig. 1).

a) GeneChip® RAE 230 2.0 probe arrays were used in all samples.
b) Two types of glutathione depletors, PHO (forming conjugation with glutathione) and BSO (glutathione synthesis inhibitor) types were used to distinguish the mechanisms of depletion.
c) Two periods for glutathione depletion were selected, i.e., the time during glutathione depletion and that after glutathione depletion. The former might reflect direct changes due to glutathione

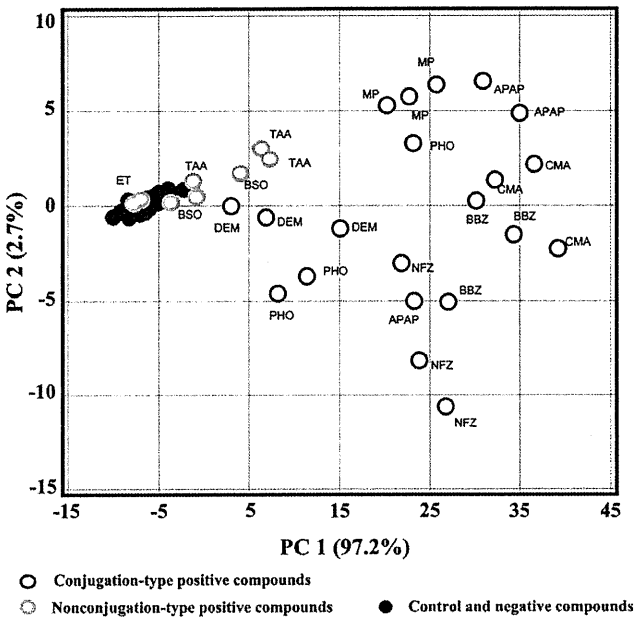

Fig. 3. Principal component analysis of gene expression profiles of the three probe sets that were found to be always upregulated during and after the time when glutathione was depleted through conjugation. PCA was performed on the data sets from the control and treated rat liver samples collected 24 h after treatment with the 17 compounds. The gene expression intensities with global normalization were calculated to obtain a fold change (log2 ratio) with standard deviation and were converted to Z-scores. The first two principal components are shown with the contribution rate of the component as the percentage of the total in each axis. Each point represents an individual sample. Abbreviations of each drug are shown in Table 1.

depletion, and the latter might contain additional indirect changes or the late-onset ones due to cell damage.

d) Exclude insignificant genes by using reference compounds to clarify the toxicological mechanism.
e) Combine the lists to produce markers convenient for practical use.

We first extracted significant genes that were mobilized during and after glutathione depletion induced by conjugation-type drugs. Their expression changes are simplified and illustrated in Fig. 6A. When glutathione began to decrease by conjugation (Fig. 6A, "During"), Srxn1 and sestrin, in addition to the stress marker aldo-keto reductase family 7 member 3 (Akr7a3) were upregulated. Recently, both sulfiredoxin and sestrin have been identified as key enzymes involved in the catalysis of sulfated peroxiredoxin to its reduced form (Lim et al., 2008). Sulfiredoxin is also known to catalyze deglutathionylation of proteins formed under oxidative stress (Findlay et al., 2006). In that paper, it was reported that protein tyrosine phosphatase 1B was identified as a target of Srxn1-dependent deglutathionylation. Srxn1-dependent deglutathionylation is known to be functionally relevant through restoration of phosphatase activity. The presented results indicate that the earliest response of hepatocytes to glutathione conjugation was the system related to sulfiredoxin/sestrin. Another marked change was the upregulation of tribbles homolog 3 (Trib3), also termed neuronal cell death-inducible putative kinase (NIPK). This gene has been reported to be upregulated when disulfide bonds of proteins were disrupted in the cell lines of human hepatocytes (Ord and Ord, 2005) and rat thyrocytes (Park et al., 2003). More recently, Trib3 was suggested to be a negative feedback regulator of ATF4-dependent transcription and to protect cells from various types of stress (Jousse et al., 2007; Ord et al., 2007). The importance of Srxn1 for the prompt compensation of reduced glutathione and early stress responses is due to the roles of Akr7a3 and Trib3.

At a certain time after glutathione depletion (Fig. 6A, "After"), some of the genes related to stress response such as Akr7a3 and Trib3 were still upregulated, suggesting that these probes are rather useful markers because one could detect the episode of glutathione depletion anytime after dosing. Characteristic changes after depletion occur in the genes related to glutathione metabolism, lipoprotein, and phosphotyrosine. Both catalytic and modifier subunits of glutamate cysteine ligase, as well as glutathione S transferases were upregulated. This appears to be a reasonable compensatory response to glutathione depletion. The lipoprotein-related genes reelin, apolipoprotein L2, and low-density lipoprotein receptor-related protein 1 (Lrp1), were downregulated. Reelin was regarded as one of the ligands of apolipoprotein E, and it is involved in various neuronal functions (Herz and Ying Chen, 2006). More recently, reelin was shown to be synthesized and secreted from hepatic stellate cells during liver injury (Botella-Lopez et al., 2008), although its expression was found to be decreased in this study. As lipid metabolism is known to be affected in the early stage of liver damage (Treinen-Molsen, 2001), these changes might be a reflection of the initiation of cell damage. Lrp1 has been reported to bind various proteins in a phosphorylation-specific manner, and subsequently, it associates with and modulates the activity of other transmembrane proteins such as receptor tyrosine kinases (Lillis et al., 2008). Actually, protein tyrosine phosphatase receptor type f and d (Ptprf and Ptprd) were found to be downregulated. It is of interest that tyrosine kinase-related events occur both during and after glutathione depletion. Further study is necessary to clarify the relationship between the downregulation of lipoprotein and proteins and tyrosine phosphorylation in the early stage of hepatocyte damage induced by glutathione depletion.

In the second step, we tried to extract significant genes that were mobilized during and after glutathione depletion induced by the inhibition of glutathione synthesis. As specific inhibitors other than BSO were not easily obtained, we could not ensure reliability of the data from multiple compounds. We searched for appropriate

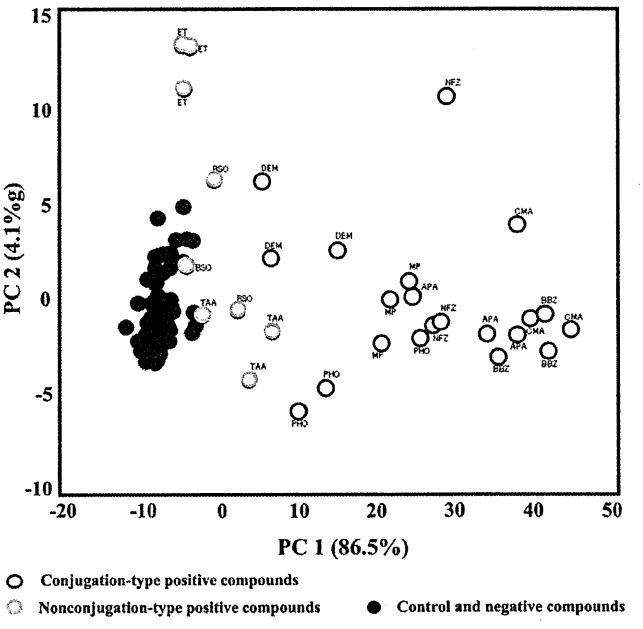

Fig. 4. Principal component analysis of gene expression profiles of the 14 probe sets mobilized during and after glutathione depletion through conjugate or enzyme inhibition is shown. PCA was performed on the data sets from the control and treated rat liver samples collected 24 h after treatment with the 17 compounds. The procedure was the same as that in Fig. 3.

A

	3 hr Low	3 hr Middle	3 hr High	6 hr Low	6 hr Middle	6 hr High	9 hr Low	9 hr Middle	9 hr High	24 hr Low	24 hr Middle	24 hr High
	4.3	2.5	−0.8	39	80.9	40.2	−3.2	32.9	12	22.2		
INAH	−0.1	0	−0.1	0.7	0.6	−6.8	2.1	−0.3	1.1	−2.4	−8.3	−2.5
TAA	−0.8	0.3	1.2	0	1.7	1.9	−3.3	0.7	1.2	3.1	76.7	166.8
ET	−1.4	−7.4	−0.9	−3.9	−8	−16	−2.1	−0.4	−0.6	−0.9	0	5.6
HCB	0.7	0.6	0	2.7	1.2	1.9	3	2.2	−0.1	0.5	15.7	0
	0.2	2.9	72.3	3	45.1		2.5	15.5	301.1	−0.4	2.3	
	56.7	26.6	2.6	145.1	197.2	−0.1	232.8			30.1		
	27.5	31.8	163.7	39.3			80.3	327.9		206.9	26.4	
PH	0.3	1.7	4.6	1.7	−0.1	−22	12.4	7.4	2.2	0.1	−0.6	0.3
GBC	−4	−0.3	−0.1	−8.2	−7.1	0.2	0.2	−1.2	0.1	−6.5	−4.6	0.6
	57.7		155.3	113.6			175.5			4.5		
EME	0	0	−0.1	1.8	−0.3	6.3	−6.5	−1.2	−1.4	−0.5	4.3	0.7
PEN	−4.1	0.6	−0.6	17.8	0.3	13.6	−0.1	5.2	11.9	−0.9	−0.2	−0.2
	27.9			128.9			89.3			1.2	117.5	
BSO	0.6	0.1	0.7	−0.1	−0.2	0.1	6.1	3.2	26.8	1.4	−1.3	35.8
	42.4			154.3			38.2			3.7	84	
GMC	−0.1	0	−0.5	−0.2	5.9	21.2	0.2	0.3	−1.6	2.3	0.7	−0.2

Probe set ID	Gene name	Gene symbol
1368121_at	aldo-keto reductase family 7, member A3 (aflatoxin aldehyde reductase)	Akr7a3
1386321_s_at	tribbles homolog 3 (Drosophila)	Trib3
1388122_at	glutathione-S-transferase, pi 1	Gstp1

B

	3 hr Low	3 hr Middle	3 hr High	6 hr Low	6 hr Middle	6 hr High	9 hr Low	9 hr Middle	9 hr High	24 hr Low	24 hr Middle	24 hr High
	−0.1	0	−5.6	7.9	7.8	1.5	−3.8	2.9	−0.5	32.9		
INAH	0	0.1	−0.8	−0.2	−0.2	−3.4	2.1	−0.2	−0.1	−1.3	−1.5	−2.3
TAA	−11.8	−0.7	2.3	0.1	1.5	−7.9	−0.4	1.6	1.6	6.4	51.9	61
ET	−5.7	−9.1	−28.8	−14.2	−23.1	−51.2	3	1.8	3.9	−1.2	3.6	37.4
HCB	1.1	1.8	0.8	2.5	4.1	0.7	2	2.2	−0.2	1.7	13.2	0.8
	11.1	3.7	7.5	1.3	36.4		2	34.2		−1.4	0.8	120.4
	31.7	4.8	0.3	130.1		−1.1			133.2	27.2		
	17.8	31.4	17.2	13.4	21.3	14.5	37.6	58.6	107.2	89.3	7.2	
PH	0.1	0.2	2.3	−0.7	−0.8	−14.2	4.8	6.7	−0.8	−0.2	−0.2	0
GBC	−0.1	1.1	−0.4	−2.3	−1.3	−0.1	−0.2	−1.7	0.3	−2.6	−3.8	0.1
	2	21.5	8.9	79.1			60.9			4.4		
EME	−0.2	−0.1	−0.5	−2	−0.2	−1.6	−7.8	−6.1	−7	−0.4	0.1	0.5
PEN	−4	1.6	−1.2	0.7	−2.3	−18.3	−0.1	3.8	−1	−0.5	−0.5	0.4
	2.9	73	34.9	78.8			34			0.2	63.5	
BSO	0.6	0.7	0	0.4	−3.6	0.5	−0.9	−26.8	4	3.3	7.5	56.2
	2.5	27.9	120.6	133.2			22.4			1.3	44.4	
GMC	−0.4	−0.3	−0.6	−0.2	0.4	−2.8	0.4	−0.2	0	−0.7	1.1	−1.5

Probe set ID	Gene name	Gene symbol
1368121_at	aldo-keto reductase family 7, member A3 (aflatoxin aldehyde reductase)	Akr7a3
1370030_at	glutamate cysteine ligase, modifier subunit	Gclm
1370688_at	glutamate-cysteine ligase, catalytic subunit	Gclc
1381968_at	cellular repressor of E1A-stimulated genes	Creg1
1387022_at	aldehyde dehydrogenase family 1, member A1	Aldh1a1
1388122_at	glutathione-S-transferase, pi 1	Gstp1

C

	3 hr Low	3 hr Middle	3 hr High	6 hr Low	6 hr Middle	6 hr High	9 hr Low	9 hr Middle	9 hr High	24 hr Low	24 hr Middle	24 hr High
APAP	−0.2	−2	−5.7	−0.1	−0.9	−1.4	0	−3.9	−6.5	−1.2	−7.6	−18.5
INAH	0.8	−0.1	0.4	0.1	0	−1	0	−0.3	−0.2	0.1	−0.2	−1.2
TAA	−2.8	−0.5	0.3	−0.4	−6	−75.2	−0.5	−1.6	−4	0.4	−0.4	−0.9
ET	−2.2	0.5	−0.8	−1.6	−10.8	−21.4	−0.3	1.2	7.4	0.2	0.7	0
HCB	−0.5	−0.5	−1.1	−2.1	−0.6	0.2	−1.2	−0.6	0.3	−0.2	−0.7	−0.5
MP	0	−0.6	−0.8	−0.5	−2.6	−52.5	0	0.2	−16.3	0	−5.2	−27.5
PHZ	−4.9	−1	−1.5	−1.3	−3.5	−7	−1.8	−21.2	−34.6	−0.2	−8.6	−34.5
CMA	−1.1	−7.2	−8.3	−8	−34	−114	−1.7	−11.3	−55.2	−0.3	−4.3	−52.3
PH	0	−1.3	−3.3	0.1	−0.4	0.4	−0.8	−0.2	−3.1	0	0	0.1
GBC	−0.5	−1.1	−1.8	0.1	−1.7	−2	0.3	1.7	0.9	0	0	0
NFZ	0	−2.9	−2.4	−1.4	−8.3	−22.3	−3	−28.6	−78.5	−0.1	−0.5	−1.5
EME	−0.1	0	−1.5	−0.4	−0.5	−2.3	−0.2	−4	−2.9	0	0	−0.2
PEN	−0.9	−3	−0.7	0	−0.3	−1.1	0.1	1.2	0	0.2	0.9	0.2
PHO	−0.4	−3	−10.9	−1.9	−13.8	−41.2	−0.5	−18.8	−26.6	−1.5	−4	−23.1
BSO	−0.5	0.3	−0.1	0	−1.2	−4.5	−17	−4.4	−5.4	0	−0.1	−1.3
DEM	0.7	−1	−18.7	−1.1	−7.7	−61.2	−1	−4.4	−85	−0.5	−4.2	−42.8
GMC	−0.1	−1.4	−0.8	0.5	0	0.4	0	−0.2	−0.6	0.1	−2	−0.8

Probe set ID	Gene name	Gene symbol
1368009_at	glucosamine	Gne
1368036_at	protein tyrosine phosphatase, receptor type, F	Ptprf
1372889_at	Transcribed locus	—
1377013_at	—	—
1379900_at	Transcribed locus	—
1383425_at	complement component 5	C5
1388416_at	low density lipoprotein receptor-related protein 1	Lrp1
1388425_at	OAF homolog (Drosophila)	Oaf

Fig. 5. A: Heat map of the TGP1 score calculated for the gene expression data of the three probe sets (shown as a table at the bottom) responding to glutathione depletion through conjugation. B: Heat map of the TGP1 score calculated for the 6 upregulated probe sets out of the 14 sets (shown as a table at the bottom) that were mobilized during and after glutathione depletion through either conjugate or enzyme inhibition. C: Heat map of the TGP1 score calculated for the 8 downregulated probe sets out of the 14 sets (shown as a table at the bottom) that were mobilized during and after glutathione depletion through either conjugate or enzyme inhibition. Compounds with magenta, orange, and white indicate conjugate-type, nonconjugate-type, and negative compounds, respectively. Calculated TGP1 scores (see Materials and methods) are indicated in the corresponding column with red for increasing and blue for decreasing direction. The actual screen images in our system (TG-GATEs) were modified for presentation.

compounds in our database and picked up ET. This compound was reported to deplete hepatic glutathione in cell suspension (Waterfield et al., 1998), and it is reasonable to attribute its mechanism to inhibition of protein synthesis, considering its antagonism toward methionine. However, ET was classified as producing a negative or a very weak, positive response in our study. This might be due to the difference in the mechanism of depletion, i.e., BSO specifically inhibits gamma-glutamylcysteine ligase, whereas ET generally inhibits de novo protein synthesis. We considered that introduction of compounds with uncertain mechanisms would not improve but could disturb the analysis. We then changed the strategy such that gene selection was based on BSO alone, and other compounds were used as reference.

Expression changes characteristic of BSO are illustrated as Fig. 6B. When glutathione starts to decrease by synthesis inhibition (Fig. 6B, "During"), Srxn1 was also upregulated as in the conjugation-type. Among the genes related to stress, heme oxygenase I (Hmox1) was upregulated, but other changes were not obvious in this case. Instead, downregulation of some genes related to lipid metabolism, such as Pcsk9, Fasn, and Scd1 (Jeong et al., 2008), was observed. At a certain time after glutathione depletion by synthesis inhibition (Fig. 6B, "After"), genes related to transporters including UST4r and SLC9, the ER-stress inducible gene, Sdf2l1 (Fukuda et al., 2001), and the interferon inducible gene, Isg20 (Espert et al., 2003), were upregulated. Other categories of genes related to cell–cell interaction (e.g., Extl1, Antxr2 and Cav2) and DNA synthesis (e.g., Zfp367, Zbtb7b, and Iroquois related homeobox1) were mobilized, but their direction varied. It appears that the population of mobilized genes was quite different between these two types of glutathione depletion. However, the fact that the marker genes extracted from the experiments using BSO separated not only enzyme inhibition-type compounds but also conjugation-type ones on PCA suggested that genes mobilized by inhibition of glutathione synthesis were not specific for this type but were also mobilized by conjugation-type compounds. In other words, the events induced by glutathione depletion were common in both types, but conjugation of glutathione could cause additional events leading to changes that are more prominent. An interesting point is that a transient increase in Srxn1 was common in these two types, suggesting a key role in the early protection of hepatocytes from oxidative stress due to glutathione depletion.

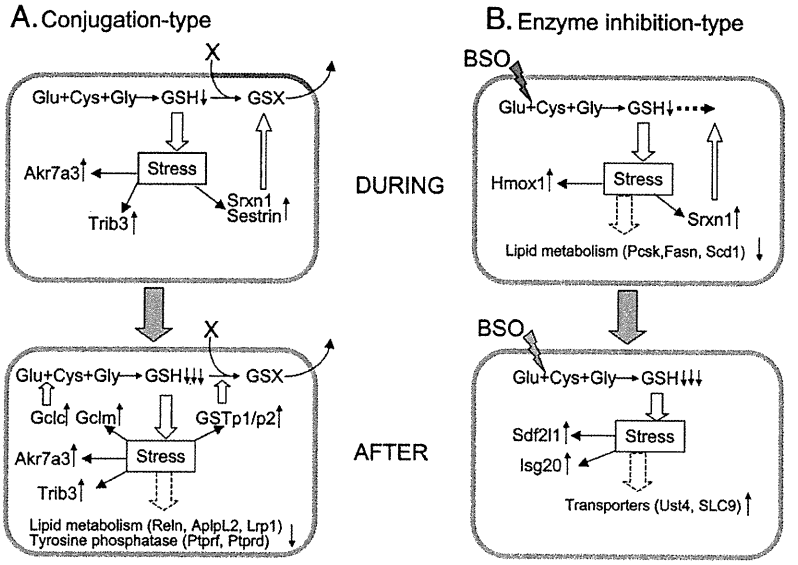

Fig. 6. Schematic representation of the events during and after depletion of glutathione in the hepatocyte by conjugation (A) or inhibition of enzyme synthesis (B).

Figs. 6A and B indicate that the gene expression profile varied depending upon the time and dose level. Although these genes are useful for elucidating the mechanism of action, the use of these for prediction or diagnosis of hepatotoxicity of a new compound is somewhat inconvenient because the dose and time are limited in usual toxicological examinations. As a result, it is impossible to know the optimal condition without preliminary tests. To improve this issue, we prepared two gene lists. Marker V consists of three genes, i.e., Akr7a3, Trib3 and Gstp1, which are considered as the most robust marker genes for hepatotoxicity induced by glutathione depletion through glutathione conjugation regardless of the time range. Marker VI consists of 14 probe sets that are useful biomarkers for hepatotoxicity induced by glutathione depletion regardless of the depleting mechanism or time. Each list, or their combination, would be useful markers for predicting the risk of glutathione depletion by chemicals under toxicological examination.

Acknowledgments

This work was supported in part by grants from the Ministry of Health, Labour and Welfare of Japan, H14-Toxico-001 and H19-Toxico-001.

Appendix A. Supplementary data

Supplementary data associated with this article can be found, in the online version, at 10.1016/j.taap.2010.06.015.

References

Botella-Lopez, A., de Madaria, E., Jover, R., Bataller, R., Sancho-Bru, P., Candela, A., Compañ, A., Pérez-Mateo, M., Martinez, S., Sáez-Valero, J., 2008. Reelin is overexpressed in the liver and plasma of bile duct ligated rats and its levels and glycosylation are altered in plasma of humans with cirrhosis. Int. J. Biochem. Cell Biol. 40, 766–775.

Dahlin, D.C., Miwa, G.T., Lu, A.Y., Nelson, S.D., 1984. N-acetyl-p-benzoquinone imine: a cytochrome P-450-mediated oxidation product of acetaminophen. Proc. Natl. Acad. Sci. U. S. A. 81, 1327–1331.

Espert, L., Degols, G., Gongora, C., Blondel, D., Williams, B.R., Silverman, R.H., Mechti, N., 2003. ISG20, a new interferon-induced RNase specific for single-stranded RNA, defines an alternative antiviral pathway against RNA genomic viruses. J. Biol. Chem. 278, 16151–16158.

Findlay, V.J., Townsend, D.M., Morris, T.E., Fraser, J.P., He, L., Tew, K.D., 2006. A novel role for human sulfiredoxin in the reversal of glutathionylation. Cancer Res. 66, 6800–6806.

Fukuda, S., Sumii, M., Masuda, Y., Takahashi, M., Koike, N., Teishima, J., Yasumoto, H., Itamoto, T., Asahara, T., Dohi, K., Kamiya, K., 2001. Murine and human SDF2L1 is an endoplasmic reticulum stress-inducible gene and encodes a new member of the Pmt/rt protein family. Biochem. Biophys. Res. Commun. 280, 407–414.

Griffith, O.W., 1981. Depletion of glutathione by inhibition of biosynthesis. Methods Enzymol. 77, 59–63.

Herz, J., Ying Chen, Y., 2006. Reelin, lipoprotein receptors and synaptic plasticity. Nat. Rev. Neurosci. 7, 850–859.

Jeong, H.J., Lee, H.-S., Kim, K.-S., Y.-K., Yoon, D., Sahng Wook Park, S.W., 2008. Sterol-dependent regulation of proprotein convertase subtilisin/kexin type 9 expression by sterol regulatory element-binding protein-2. J. Lipid Res. 49, 399–409.

Jousse, C., Deval, C., Maurin, A.C., Parry, L., Chérasse, Y., Chaveroux, C., Lefloch, R., Lenormand, P., Bruhat, A., Fafournoux, P., 2007. TRB3 inhibits the transcriptional activation of stress-regulated genes by a negative feedback on the ATF4 pathway. J. Biol. Chem. 282, 15851–15861.

Kiyosawa, N., Ito, K., Sakuma, K., Niino, N., Kanbori, M., Yamoto, T., Manabe, S., Matsunuma, N., 2004. Evaluation of glutathione deficiency in rat livers by microarray analysis. Biochem. Pharmacol. 68, 1465–1475.

Kiyosawa, N., Shiwaku, K., Hirode, M., Omura, K., Uehara, T., Shimizu, T., Mizukawa, Y., Miyagishima, T., Ono, A., Nagao, T., Urushidani, T., 2006. Utilization of a one-dimensional score for surveying the chemical-induced changes in expression levels of multiple biomarker gene sets using a large-scale toxicogenomics database. J. Toxicol. Sci. 31, 433–448.

Kiyosawa, N., Uehara, T., Gao, W.-H., Omura, K., Hirode, M., Shimizu, T., Mizukawa, Y., Ono, A., Miyagishima, T., Nagao, T., Urushidani, T., 2007. Identification of glutathione depletion-responsive genes using phorone-treated rat liver. J. Toxicol. Sci. 32, 469–486.

Lake, B.G., Gray, T.J., Evans, J.G., Lewis, D.F., Beamand, J.A., Hue, K.L., 1989. Studies on the mechanism of coumarin-induced toxicity in rat hepatocytes: comparison with dihydrocoumarin and other coumarin metabolites. Toxicol. Appl. Pharmacol. 97, 311–323.

Lillis, A.P., Van Duyn, L.B., Murphy-Ullrich, J.E., Strickland, D.K., 2008. LDL receptor-related protein 1: unique tissue-specific functions revealed by selective gene knockout studies. Physiol. Rev. 88, 887–918.

Lim, J.C., Choi, H.I., Park, Y.S., Nam, H.W., Woo, H.A., Kwon, K.S., Kim, Y.S., Rhee, S.G., Kim, K., Chae, H.Z., 2008. Irreversible oxidation of the active-site cysteine of peroxiredoxin to cysteine sulfonic acid for enhanced molecular chaperone activity. J. Biol. Chem. 283, 28873–28880.

Lu, S.C., 1999. Regulation of hepatic glutathione synthesis: current concepts and controversies. FASEB J. 13, 1169–1183.

Mesa, M.L., Carrizosa, R., Martinez-Honduvilla, C., Benito, M., Fabregat, I., 1996. Changes in rat liver gene expression induced by thioacetamide: protective role of S-adenosyl-L-methionine by a glutathione-dependent mechanism. Hepatology 23, 600–606.

Ord, D., Ord, T., 2005. Characterization of human NIPK (TRB3, SKIP3) gene activation in stressful conditions. Biochem. Biophys. Res. Commun. 330, 210–218.

Ord, D., Meerits, K., Ord, T., 2007. TRB3 protects cells against the growth inhibitory and cytotoxic effect of ATF4. Exp. Cell Res. 313, 3556–3567.

Park, S., Hwang, I., Shong, M., Kwon, O.Y., 2003. Identification of genes in thyrocytes regulated by unfolded protein response by using disulfide bond reducing agent of dithiothreitol. J. Endocrinol. Invest. 26, 132–137.

Plummer, J.L., Smith, B.R., Sies, H., Bend, J.R., 1981. Chemical depletion of glutathione in vivo. Methods Enzymol. 77, 50–59.

Ratra, G.S., Powell, C.J., Park, B.K., Maggs, J.L., Cottrell, S., 2000. Methapyrilene hepatotoxicity is associated with increased hepatic glutathione, the formation of glucuronide conjugates, and enterohepatic recirculation. Chem. Biol. Interact. 129, 279–295.

Soga, T., Baran, R., Suematsu, M., Ueno, Y., Ikeda, S., Sakurakawa, T., Kakazu, Y., Ishikawa, T., Robert, M., Nishioka, T., Tomita, M., 2006. Differential metabolomics reveals ophthalmic acid as an oxidative stress biomarker indicating hepatic glutathione consumption. J. Biol. Chem. 281, 16768–16776.

Sorrentino, D., Bode, W., Hoener, B.A., 1987. Nitrofurazone disposition by perfused rat liver. Effect of dose size and glutathione depletion. Biochem. Pharmacol. 36, 915–918.

Treinen-Molsen, M., 2001. Toxic responses of the liver. In: Klaassen, C.D. (Ed.), Casarett and Doull's Toxicology. McGraw-Hill, New York, pp. 471–489.

Urushidani, T., 2007. Prediction of hepatotoxicity based on the toxicogenomics database. In: Sahu, Saura C. (Ed.), Hepatotoxicity. Wiley-VCH, pp. 507–529.

van Doorn, R., Leijdekkers, C.M., Henderson, P.T., 1978. Synergistic effects of phorone on the hepatotoxicity of bromobenzene and paracetamol in mice. Toxicology 11, 225–233.

Waterfield, C.J., Westmoreland, C., Asker, D.S., Murdock, J.C., George, E., Timbrell, J.A., 1998. Ethionine toxicity in vitro: the correlation of data from rat hepatocyte suspensions and monolayers with in vivo observations. Arch. Toxicol. 72, 588–596.

DOI 10.1002/mnfr.200900169 *Mol. Nutr. Food Res.* 2010, *54*, 218–227

REVIEW

The Japanese toxicogenomics project: Application of toxicogenomics

Takeki Uehara[1,2], Atsushi Ono[2,3], Toshiyuki Maruyama[1], Ikuo Kato[1], Hiroshi Yamada[2], Yasuo Ohno[2,3] and Tetsuro Urushidani[2,4]

[1] Developmental Research Laboratories, Shionogi & Co., Ltd., Futaba-cho, Toyonaka, Osaka, Japan
[2] Toxicogenomics Informatics Project, National Institute of Biomedical Innovation, Asagi, Ibaraki, Osaka, Japan
[3] National Institute of Health Sciences, Kamiyoga, Setagaya-ku, Tokyo, Japan
[4] Department of Pathophysiology, Faculty of Pharmaceutical Sciences, Doshisha Women's College of Liberal Arts, Kodo, Kyotanabe, Kyoto, Japan

Biotechnology advances have provided novel methods for the risk assessment of chemicals. The application of microarray technologies to toxicology, known as toxicogenomics, is becoming an accepted approach for identifying chemicals with potential safety problems. Gene expression profiling is expected to identify the mechanisms that underlie the potential toxicity of chemicals. This technology has also been applied to identify biomarkers of toxicity to predict potential hazardous chemicals. Ultimately, toxicogenomics is expected to aid in risk assessment. The following discussion explores potential applications and features of the Japanese Toxicogenomics Project.

Received: April 13, 2009
Revised: July 29, 2009
Accepted: August 6, 2009

Keywords:
Genomic biomarker / Hepatotoxicity / Microarray / Toxicogenomics Project / Toxicogenomics

1 Introduction

Today, in the post-genomic era, there have been remarkable advances in the technology of drug development. Drug development in the previous century was usually based on screening the effects of chemicals in model animals with artificially created diseases; subsequently, it sometimes happened that an excellent drug was produced not for humans, but for rats. In recent years, however, it has been possible to start the development process by targeting disease-related genes whose molecular functions are well elucidated, and indeed, human genes are always available. Therefore, it is now easy to select a chemical that is effective on the human molecule on at least the *in vitro* level. Even with this advantage, many candidate drugs have been eliminated because of toxicity that could not be found in preclinical tests in the early stage of drug development; rather, the toxicity became apparent at the later stage of drug development, such as during long-term toxicity studies for animal models and after several stages of clinical trials [1]. In extreme cases, serious adverse effects emerge even after the drugs are widely distributed on the world market. A top priority should be the solution of this paradox; *i.e.* how to predict "unpredictable" toxicity. The response of the organism to the toxicant that subsequently causes pathological changes in certain organs with a low dose should be detectable as changes in the expression of genes, protein synthesis, and metabolism. Of these changes, the expression of genes, or the amount of mRNA, is the most sensitive measure and one of the largest advantages in the technology of genomics. Therefore, toxicogenomics, which enables us to comprehensively analyze gene expression changes caused by an external stimulus in a specific organ, is considered to

Correspondence: Dr. Takeki Uehara, Developmental Research Laboratories, Shionogi & Co., Ltd., 3-1-1 Futaba-cho, Toyonaka, Osaka 561-0825, Japan
E-mail: takeki.uehara@shionogi.co.jp
Fax: +81-6-6332-6385

Abbreviations: BSO, L-buthionine-S,R-sulfoximine; **PAM,** prediction analysis of microarray; **PCA,** principal component analysis; **PPARα,** peroxisome proliferator-activated receptor alpha; **PSTC,** Predictive Safety Testing Consortium; **SVM,** support vector machine; **TGP,** Toxicogenomics Project

be one of the most powerful strategies. In particular, the identification of predictive biomarkers for drug-induced toxicity at or before the pre-clinical stages of drug development is of great importance to pharmaceutical companies.

2 Current status of worldwide toxicogenomics database creation

To appropriately interpret the microarray data, it is desirable to perform comparative analyses with data obtained from prototypical toxicants. Moreover, toxicogenomics studies are built on standard toxicology studies, and one goal of toxicogenomics is to detect relationships between changes in gene expression and toxicological end-point data, such as histopathology, clinical chemistry, and other toxicity data. Therefore, a large-scale, high-quality, and well-designed toxicogenomics database of gene expression information and standard toxicological data are essential. Several public toxicogenomic database efforts have been initiated, such as Gene Expression Omnibus [2, 3] (GEO; National Center for Biotechnology Information, National Institutes of Health; www.ncbi.nlm.nih.gov/geo), ArrayExpress [4, 5] (European Bioinformatics Institute; www.ebi.ac.uk/microarray-as/ae/), Center for Information Biology Gene Expression [6] (CIBEX; DNA Data Bank of Japan, National Institute of Genetics; http://cibex.nig.ac.jp/), EDGE (McArdle Laboratory for Cancer Research [7], University of Wisconsin-Madison; http://edge.oncology.wisc.edu/edge3.php), Chemical Effects in Biological Systems [8] (CEBS; National Institute of Environmental Health Sciences; http://cebs.niehs.nih.gov/cebs-browser/), dbZach [9] (Department of Biochemistry & Molecular Biology, Michigan State University; http://dbzach.fst.msu.edu), and Comparative Toxicogenomics Database [10, 11] (CTD; Mount Desert Island Biological Laboratory; http://ctd.mdibl.org).

In addition to these public microarray databases, public consortia provide a forum to address questions requiring more resources than one organization alone could provide and to engage many sectors of the scientific community. InnoMed PredTox [12] is a joint Industry and European Commission collaboration to improve drug safety. The consortium is a collaborative project of 15 research groups from 12 pharmaceutical companies, three academic institutions and two technology providers. The goal of this consortium is to assess the value of combining results from "omics" technologies (transcriptomics, proteomics, metabolomics) with results from more conventional toxicology methods for more informed decision making in pre-clinical safety evaluation. Genedata (http://www.genedata.com/), a company that offers expertise in research informatics combined with open and scalable computational solutions, has provided the computational infrastructure for InnoMed PredTox, in particular the software for data management and analysis.

The Liver Toxicity Biomarker Study [13] is a collaborative pre-clinical research effort in molecular systems toxicology between the National Center for Toxicological Research and BG Medicine and it is supported by seven pharmaceutical companies and three technology providers. The Liver Toxicity Biomarker Study is an innovative approach to investigate drug-induced liver injury because it compares molecular events produced *in vivo* by compound pairs that (i) are similar in structure and mechanism of action, (ii) are associated with few or no signs of liver toxicity in pre-clinical studies, and (iii) show marked differences in hepatotoxic potential.

In Japan, the Toxicogenomics Project (TGP) has established a large-scale toxicogenomics database known as TG-GATEs [Genomics-Assisted Toxicity Evaluation System developed by the TGP in Japan]. Several genomic candidate biomarkers to predict the toxicity of chemicals have been successfully identified by using our database. The work and results reviewed here focuses on our efforts in toxicogenomics research and highlights recent progress in the application of toxicogenomics.

3 The TGP in Japan

3.1 Features of the project

The Ministry of Health, Labour and Welfare, National Institute of Health Sciences (NIHS), and the working group of Japan Pharmaceutical Manufacturers Association planned the TGP, a collaborative project of the government and private companies. The TGP was a 5-year project (2002–2007) performed by National Institute of Health Sciences, 15 pharmaceutical companies (Astellas, Chugai, Daiichi, Dainippon-Sumitomo, Eisai, Kissei, Mitsubishi, Mochida, Ono, Otsuka, Sankyo, Sanwa, Shionogi, Takeda, Tanabe) and the National Institute Biomedical Innovation (NIBIO), which was the core institute where the actual work was performed. Half of the budget was provided by a grant from the Ministry of Health, Labour and Welfare, and the other half was provided by the pharmaceutical companies.

The primary goal of the TGP was to create a gene expression database by using the Affymetrix GeneChip® of 150 chemicals, mainly medical drugs (Table 1), and the main target organ was the liver. Most clinically serious adverse effects occur in the liver, and the cell-type composition of the liver is relatively homogenous; thus, the expected variation based on sampling differences would be minimal. For these reasons, the liver was selected as the target organ to accumulate know-how regarding the toxicogenomics technique. Nephrotoxicity was also considered to be important; therefore, the kidney, in addition to the liver, was sampled for microarray analysis and pathologically examined in all the animals.

The TGP was completed in 2007. The entire system consists of a database, an analysis system, and a prediction system and is named as TG-Genomics-Assisted Toxicity

Table 1. Chemicals selected (in total 150 compounds) in TGP

Acetaminophen	Doxorubicin hydrochloride	Nitrofurantoin
Acetazolamide	D-Penicillamine	Nitrofurazone
Ajmaline	Enalapril maleate	N-nitrosodiethylamine
Allopurinol	Erythromycin ethylsuccinate	N-phenylanthranilic acid
Allyl alcohol	Ethambutol dihydrochloride	Omeprazole
Alpha-naphthyl isothiocyanate	Ethanol	Papaverine hydrochloride
Amiodarone hydrochloride	Ethionamide	Pemoline
Amitriptyline hydrochloride	Etoposide	Perhexiline maleate
Aspirin	Famotidine	Phenacetin
Azathioprine	Fenofibrate	Phenobarbital sodium
Bendazac	Fluphenazine dihydrochloride	Phenylbutazone
Benzbromarone	Flutamide	Phenytoin
Benziodarone	Furosemide	Promethazine hydrochloride
Bromobenzene	Gemfibrozil	Propylthiouracil
Bucetin	Gentamicin sulfate	Puromycin aminonucleoside
Caffeine	Glibenclamide	Quinidine sulfate
Captopril	Griseofulvin	Ranitidine hydrochloride
Carbamazepine	Haloperidol	Rifampicin
Carbon tetrachloride	Hexachlorobenzene	Simvastatin
Carboplatin	Hydroxyzine dihydrochloride	Sodium valproate
Cephalothin sodium	Ibuprofen	Sulfasalazine
Chloramphenicol	Imipramine hydrochloride	Sulindac
Chlormadinone acetate	Indomethacin	Tacrine hydrochloride
Chlormezanone	Iproniazid phosphate	Tamoxifen citrate
Chlorpromazine Hydrochloride	Isoniazid	Tannic acid
Chlorpropamide	Ketoconazole	Terbinafine hydrochloride
Cimetidine	Labetalol hydrochloride	Tetracycline hydrochloride
Ciprofloxacin hydrochloride	Lomustine	Theophylline
Cisplatin	Lornoxicam	Thioacetamide
Clofibrate	Mefenamic acid	Thioridazine hydrochloride
Clomipramine hydrochloride	Meloxicam	Ticlopidine hydrochloride
Colchicine	Metformin hydrochloride	Tiopronin
Coumarin	Methapyrilene hydrochloride	Tolbutamide
Cyclophosphamide monohydrate	Methimazole	Triamterene
Cyclosporine A	Methotrexate	Triazolam
Danazol	Methyldopa	Trimethadione
Dantrolene sodium Hemiheptahydrate	Methyltestosterone	Vancomycin hydrochloride
Diazepam	Mexiletine hydrochloride	Vitamin A
Diclofenac sodium	Monocrotaline	WY-14,643
Diltiazem hydrochloride	Moxisylyte hydrochloride	(±)-Chlorpheniramine maleate
Disopyramide	Naproxen	(±)-Sulpiride
Disulfiram	Nicotinic acid	17-alpha-Ethinyl estradiol
DL-ethionine	Nifedipine	2-Acetamidofluorene
Doxepin hydrochloride	Nimesulide	2-Bromoethylamine hydrobromide

Drug candidates supplied from the member companies, which were withdrawn in various stages of drug development, were excluded.

Evaluation System. The database will be available to the public in the near future.

3.2 Contents of the database

Our standard study protocol is summarized in Table 2.

In vivo study: The rat was selected as the species for analysis. Rats were very frequently used in non-clinical examinations, and toxicological information for the rat has been accumulated. Both a single-dose study, consisting of multiple time points with multiple dose levels, and a repeated-dose study, consisting of multiple dose periods with multiple dose levels, were performed. Data obtained from each animal included body weight, general symptoms, hematology, blood biochemistry, organ weight, and a histopathological examination of the liver and kidney. Gene expression in the liver and kidney was comprehensively analyzed by using Affymetrix GeneChip® arrays.

In vitro study: A modified two-step collagenase perfusion method was used to isolate liver cells from 6-week-old male Sprague–Dawley rats. A comprehensive gene expression analysis was performed on the primary cultured cells at multiple time points after treatment with various concen-

Table 2. The standard study protocol in TGP

In vivo	
Animal	Sprague–Dawley rat (6 wk old, $N = 5$ for each group)
Vehicle	0.5% Methylcellulose or corn oil (oral dose) Saline or 5% glucose solution (intravenous dose)
Dose	Low, middle, and high (mainly 1:3:10)
Route	Oral (intravenous in a few cases)
Sacrifice	3, 6, 9, and 24 h after a single administration 24 h after the last dose of repeated administration for 3, 7, 14 and 28 days
Sampling	Liver, kidney, and plasma
Microarray analysis	Affymetrix GeneChip ($N = 3$ for each group)
Items examined	Histopathology: liver and kidney Body weight, organ weight (liver and kidney), food consumption, hematology, and blood biochemistry
In vitro: rat	
Animal	Sprague–Dawley rat (6 weeks old)
Cell	Hepatocyte isolated by collagenase digestion
Vehicle	Culture medium or DMSO
Concentration	Low, middle, high (1:5:25)
Treatment	2, 8, 24 h
Microarray analysis	Duplicate
Items examined	Cell viability (LDH release and DNA contents)
In vitro: human	
Cell	Human frozen hepatocytes
Vehicle	Culture medium or DMSO
Concentration	Low, middle, and high (1:5:25, low is omitted in some cases)
Treatment	2, 8, 24 h (2 h is omitted in some cases)
Microarray analysis	Duplicate
Items examined	Cell viability (LDH release and DNA contents)

trations of each of the 150 compounds. The same gene expression analysis was also performed with human liver cultured cells obtained from Tissue Transformation Technologies.

3.3 Analysis and prediction systems

Analysis system: Since microarray data consist of large amounts of numerical data, statistical knowledge and computational skills are required to interpret the results. Multivariate analysis methods are utilized for both data mining and pattern recognition, such as hierarchical clustering, K-means clustering, self-organizing map (SOM), and principal component analysis (PCA). PCA is a convenient tool for the qualitative classification of compounds against a list of genes. As a prediction system, however, some quantitative data would be favorable for the final output. Therefore, in our system, when the user specifies a principal component with high contribution, the compounds are sorted by value, and the genes with large eigenvector values are easily obtained. This analysis provides the relative position of the test drug among the drugs in the database and supports to generate a candidate gene list for further investigation.

Prediction system: Discriminant analysis is a powerful technique that can be used when a phenotype that can be judged as positive or negative is available [14]. Prediction analysis of microarray (PAM) [15] and support vector machine (SVM) [16] have been employed in our systems. The sample size and appropriate selection of the training data set are crucial for establishing reliable classifiers. In our system, by a semi-automatic system of training and validation, the efficiency improves for the creation of classifiers.

BaseView system: When an assessment or prediction of toxicity is made by a list of multiple measures, it is necessary to summarize or quantify these measurements. Ideally, the quantification process should be optimized for each marker gene list. However, because this approach is practically difficult, a uniform system has to be created. In our system, a new scoring system was developed in one trial. The TGP1 score is calculated based on the ratio to control value (log 2) for each gene in the marker list and expressed as a heat map [17, 18]. This scoring system makes it easy to summarize the assessments of a target compound against many marker lists and to summarize the assessments of many compounds against a particular marker list. However, this system has some problems; the score is biased when the list contains a gene whose expression change is extremely large (*e.g.*, CYP1A1), and changes are canceled when up- and down-regulated genes coexists in the list. Therefore, another scoring system, the TGP2 score, is available in our system. The TGP2 score is based on the effect size and calculated as the absolute value of the difference between means divided by the covariance [19].

4 Application of toxicogenomics

Our strategy is to prepare a large set of genomic biomarkers that are related to toxicological phenotypes, pathways, or any other biologically meaningful factor. Until now, several potential genomic biomarkers to predict the toxicity of chemicals have been successfully identified. In this article, we provide several applications of toxicogenomics by using our database.

4.1 Glutathione depletion [20]

The hepatotoxicity of acetaminophen is caused by the excessive production of active metabolite that exceeds the detoxification capacity of intracellular glutathione [21]. Therefore, drugs that

have the potential to deplete hepatocyte glutathione carry the risk of causing acetaminophen-type hepatotoxicity with overdosage. In a previous report, a list of marker genes for glutathione depletion was extracted by using BSO, a glutathione biosynthesis inhibitor [22]. However, phorone is considered to be superior to L-buthionine-S,R-sulfoximine (BSO) as a model system, since its mechanism of glutathione depletion is similar to that of acetaminophen-type hepatotoxicants (*i.e.* it covalently binds to glutathione and is excreted from the cell). Phorone (40, 120, or 400 mg/kg) was administered according to the same protocol as the regular single-dose experiments, and the glutathione content was measured. Phorone caused a marked but transient depletion of glutathione with maximal depletion occurring at 3 h. Then, the glutathione level recovered, and it was increased at 24 h as a rebound effect. A total of 161 probe sets was identified with signal levels that were inversely correlated with the hepatic glutathione content (Fig. 1). PCA of the chemicals in the database with these probe sets revealed that chemicals with a risk of glutathione depletion, such as bromobenzene and coumarin, in addition to acetaminophen, were clearly separated from other chemicals or controls toward the direction of principal component 1, suggesting that the list was useful as a genomic biomarker for risk assessment of glutathione depletion.

4.2 Phospholipidosis [23]

In toxicity studies, phospholipidosis is often observed in various tissues including the liver. Despite efforts to establish methods to predict the phospholipidosis of drugs, sensitive diagnostic markers, and effective prognostic markers were still desired. To identify a genomic biomarker for the prediction of hepatic phospholipidosis, we extracted 78 probe sets of rat hepatic genes based on data from five drugs (amiodarone, amitriptyline, clomipramine, imipramine, and ketoconazole) that induce this phenotype. A PCA was performed, and the possible induction of phospholipidosis was predictable by the expression of these genes 24 h after a single administration.

4.3 Cholestasis [24]

Cholestatic hepatitis is the most common type of drug-induced cholestasis and is more frequent than cholestatic viral hepatitis. Cholestasis is caused by a functional defect in bile formation at the level of the hepatocyte or by an impairment in bile secretion and flow at the level of the bile ductules or ducts. To identify a biomarker for the diagnosis of elevated total and direct bilirubin, we extracted 59 probe sets of rat hepatic genes based on data from seven drugs (gemfibrozil, phalloidin, colchicine, bendazac, rifampicin, cyclosporine A, and chlorpromazine) that induce cholestatic hepatitis after 3–28 days of repeated administration. PCA with these probe sets clearly separated dose- and time-dependent clusters in the treated groups from the control groups. Although further work is required to improve and generalize the candidate for a marker suggested in this study, these identified probe sets should be useful to diagnose the cause of elevated total and direct bilirubin.

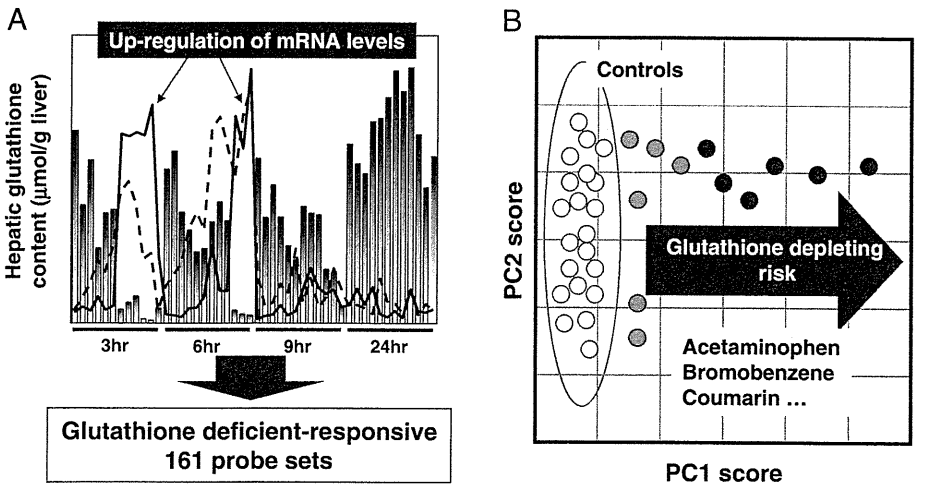

Figure 1. Identification and application of genomic biomarkers for assessing glutathione depletion. A model case for identifying the candidate genomic biomarker associated with glutathione depletion-type liver injury is presented. Rats were treated with a glutathione depletor, phorone, and microarray analysis was performed on the liver tissue. (A) A total of 161 probe sets had signal levels that were inversely correlated with the hepatic glutathione content. (B) The validity of these probe sets as biomarkers for the evaluation of glutathione depletion risk was evaluated by PCA. This evaluation revealed that chemicals with a risk of glutathione depletion, such as bromobenzene and coumarin, in addition to acetaminophen, were clearly separated from other chemicals or controls toward the direction of PC1.

4.4 Non-genotoxic hepatocarcinogenicity [25]

Assessing carcinogenicity in animals is difficult and costly; therefore, an alternative strategy is desired. Genotoxic compounds are usually identified and removed early from compound pipelines. However, the discovery of unexpected, presumed non-genotoxic, carcinogenicity late in drug development may prevent potentially good medicines from reaching patients for years while the human risk is qualified. Microarrays and expression profiling have been used to make classifiers for the early prediction of non-genotoxic carcinogenicity in the liver [26–29]. The goal of these studies was to extract common gene sets coordinately deregulated by different classes of non-genotoxic hepatocarcinogenesis. These publications confirm that multiple genes are required for accurate classification due to the multiple mechanisms of action that must be included in the prediction model. Therefore, the effects of chemicals with similar mechanisms are likely to be reflected in similar gene expression profiles in the early stage of non-genotoxic carcinogenesis [28]. Arguably more important than the identification of potential carcinogenicity of a compound is the identification of the mechanism of action [30]. Our strategy was to focus on one important mechanism, cytotoxic oxidative stress, responsible for non-genotoxic hepatocarcinogenesis.

We selected thioacetamide and methapyrilene as prototypic oxidative stress-mediated, non-genotoxic hepatocarcinogens and performed PAM discriminant analysis. A PAM classifier containing 112 probe sets that yielded an overall success rate of 95% was successfully obtained from the training procedure. Based on gene ontology, the content of genes related to cellular metabolism, including anti-oxidative metabolism, cell proliferation, cell cycle, and response to DNA damage stimulus, was significantly high. The validity of this classifier was checked for 30 chemicals. The classification results showed characteristic time-dependent increases by treatment with several non-genotoxic hepatocarcinogens, including thioacetamide, methapyrilene, coumarin, and ethionine (Fig. 2). Although all of the carbon tetrachloride-treated groups were predicted as negative, the score tended to increase with repeated dosing. On the other hand, the enzyme inducers with carcinogenic activity, phenobarbital and hexachlorobenzene, and peroxisome proliferators other than Wy-14643 (*i.e.* clofibrate and gemfibrozil) had negative scores for all time points. Of the non-carcinogenic samples, bromobenzene had a transient score increase at 24 h but returned to negative during repeated dosing. Almost all of the non-carcinogens were correctly predicted as negative, but it was not possible to completely eliminate false positives. This work suggested that the possibility of lowering the days of repeated administration to less than 28, at least for a category of non-genotoxic hepatocarcinogens causing oxidative stress.

The carcinogenicity working group of the C-Path Predictive Safety Testing Consortium (PSTC) has selected genes from published toxicogenomics research that were

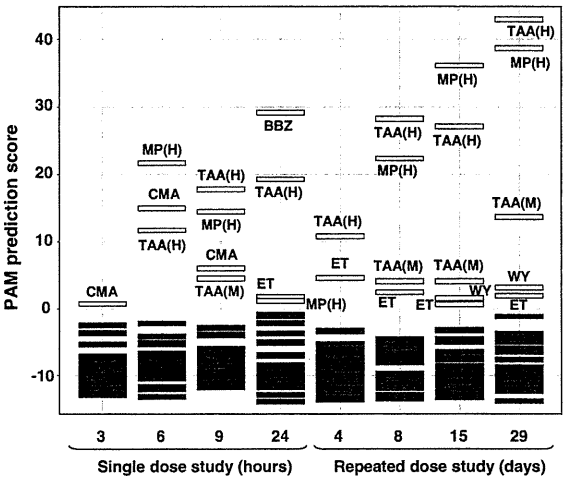

Figure 2. Time-course changes in prediction results for non-genotoxic hepatocarcinogenicity of chemicals. A model case for identifying the candidate genomic biomarkers associated with non-genotoxic hepatocarcinogenicity is presented. The PAM class probability was converted to a score to enable quantitative comparison. The PAM score showed characteristic time-course changes for several non-genotoxic hepatocarcinogens. For methapyrilene, thioacetamide and other carcinogens, such as the ethionine and coumarin, the scores transiently increased at an early time point after a single dosing. In the case of repeated dosing, the scores increased with the repeated doses. The following samples were classified as positive: methapyrilene 100 mg/kg (high dose, H); thioacetamide 15 mg/kg (middle dose, M) and 45 mg/kg (H); coumarin 150 mg/kg; ethionine 250 mg/kg; Wy-14643 100 mg/kg; and bromobenzene 300 mg/kg. Each box indicates the PAM score. Black boxes indicate samples that are predicted as negative.

determined to be of high predictive value in the early recognition of non-genotoxic hepatocarcinogenicity. The group consolidated this list for refinement and qualification as a gene signature to predict a compound's potential to be a non-genotoxic hepatocarcinogen. To ensure the independence and cost effectiveness of the platform, mRNA for these genes was assayed by real-time quantitative PCR, and a final signature was re-derived from genes with confirmed expression. The robustness and potential utility of this new quantitative PCR-based signature will be discussed in future reports.

4.5 Bridging between *in vivo* and *in vitro*: Peroxisome Proliferator-Activated Receptor alpha-mediated response [31]

Data from three ligands of peroxisome proliferator-activated receptor alpha (PPARα) – *i.e.* clofibrate, WY-14643, and gemfibrozil – in our database were analyzed. Many of the β-oxidation-related genes were commonly induced *in vivo* and *in vitro*, whereas expression changes in genes related to cell proliferation and apoptosis were detected *in vivo* but not